

Surface self-assembly of colloidal crystals for micro- and nano-patterning

van Dommelen, Ryan; Fanzio, Paola; Sasso, Luigi

DOI

[10.1016/j.cis.2017.10.007](https://doi.org/10.1016/j.cis.2017.10.007)

Publication date

2017

Document Version

Final published version

Published in

Advances in Colloid and Interface Science

Citation (APA)

van Dommelen, R., Fanzio, P., & Sasso, L. (2017). Surface self-assembly of colloidal crystals for micro- and nano-patterning. *Advances in Colloid and Interface Science*, 251 (January 2018), 97-114. <https://doi.org/10.1016/j.cis.2017.10.007>

Important note

To cite this publication, please use the final published version (if applicable). Please check the document version above.

Copyright

Other than for strictly personal use, it is not permitted to download, forward or distribute the text or part of it, without the consent of the author(s) and/or copyright holder(s), unless the work is under an open content license such as Creative Commons.

Takedown policy

Please contact us and provide details if you believe this document breaches copyrights. We will remove access to the work immediately and investigate your claim.



Historical perspective

Surface self-assembly of colloidal crystals for micro- and nano-patterning

Ryan van Dommelen, Paola Fanzio *, Luigi Sasso *

Delft University of Technology, Dept. of Precision and Microsystems Engineering (PME), Mekelweg 2, 2628 CD Delft, Netherlands



ARTICLE INFO

Available online 8 November 2017

Keywords:

Colloidal particles
Self-assembly
Nano-patterning
Polymer manufacturing

ABSTRACT

The controlled patterning of polymeric surfaces at the micro- and nanoscale offers potential in the technological development of small-scale devices, particularly within the fields of photovoltaics, micro-optics and lab- and organ-on-chip, where the topological arrangement of the surface can influence a system's power generation, optical properties or biological function - such as, in the latter case, biomimicking surfaces or topological control of cellular differentiation.

One of the most promising approaches in reducing manufacturing costs and complexity is by exploitation of the self-assembling properties of colloidal particles. Self-assembly techniques can be used to produce colloidal crystals onto surfaces, which can act as replicative masks, as has previously been demonstrated with colloidal lithography, or templates in mold-replication methods with resolutions dependent on particle size. Within this context, a particular emerging interest is focused on the use of self-assembled colloidal crystal surfaces in polymer replication methods such as soft lithography, hot and soft embossing and nano-imprint lithography, offering low-cost and high-resolution alternatives to conventional lithographic techniques.

However, there are still challenges to overcome for this surface patterning approach to reach a manufacturing reliability and process robustness comparable to competitive technologies already available in the market, as self-assembly processes are not always 100% effective in organizing colloids within a structural pattern onto the surface. Defects often occur during template fabrication. Furthermore, issues often arise mainly at the interface between colloidal crystals and other surfaces and substrates. Particularly when utilized in high-temperature pattern replication processes, poor adhesion of colloidal particles onto the substrate results in degradation of the patterning template. These effects can render difficulties in creating stable structures with little defect that are well controlled such that a large variety of shapes can be reproduced reliably.

This review presents an overview of available self-assembly methods for the creation of colloidal crystals, organized by the type of forces governing the self-assembly process: fluidic, physical, external fields, and chemical. The main focus lies on the use of spherical particles, which are favorable due to their high commercial availability and ease of synthesis. However, also shape-anisotropic particle self-assembly will be introduced, since it has recently been gaining research momentum, offering a greater flexibility in terms of patterning. Finally, an overview is provided of recent research on the fabrication of polymer nano- and microstructures by making use of colloidal self-assembled templates.

© 2017 The Authors. Published by Elsevier B.V. This is an open access article under the CC BY license (<http://creativecommons.org/licenses/by/4.0/>).

Contents

1.	Introduction	98
2.	Colloidal particles and interactions	98
2.1.	Colloidal particles	98
2.2.	Interactions between colloidal particles	99
2.2.1.	van der Waals interaction (vdW) [36,37]	99
2.2.2.	Electrostatic interaction [38,39]	99
2.2.3.	Steric effect [40]	99
2.2.4.	Capillary forces [41]	99
2.3.	DLVO theory	99
3.	Self-assembly techniques	99

* Corresponding authors.

E-mail addresses: p.fanzio-1@tudelft.nl (P. Fanzio), l.sasso@tudelft.nl (L. Sasso).

3.1.	Colloidal crystals	100
3.2.	Fluidic	101
3.2.1.	Fluidic deposition	101
3.2.2.	Droplet evaporation	101
3.3.	Physical	103
3.3.1.	Spin-coating	103
3.3.2.	Surface structuring and liquid crystal confinement	104
3.3.3.	Doctor blade: shear and gravity assisted	105
3.4.	External field	105
3.4.1.	Electric field	105
3.4.2.	Magnetic field	106
3.5.	Chemical	106
3.5.1.	Template functionalization	106
3.5.2.	Patchy particles	107
3.5.3.	DNA functionalization	107
4.	Nano-patterning with colloidal crystals	108
4.1.	Colloidal lithography	108
4.2.	Mold-replication techniques	109
5.	Conclusion and outlook	109
	Acknowledgments	113
	References	113

1. Introduction

Mold-replication techniques such as soft lithography [1,2], hot embossing [3–5] and nanoimprinting [6,7] are the most frequently used techniques for patterning polymers at small scales. Achievable resolution is high (below 100 nm) and these techniques are well established and cheap. In each case, a prefabricated pattern (master mold) is replicated into a polymeric material (target) [8]. The master is usually made out of silicon and patterned by means of a top-down method, typically by subtractive manufacturing where material is removed from the bulk, such that the desired structure remains. Photolithography is the most commonly used method to produce these masters as it is well established, mainly due to an intensive application in the high-tech industry, which has led to significant advances over the last 20 years in terms of minimally achievable resolutions. A continuous desire to scale down feature sizes has allowed the fabrication of structures with sub 10 nm feature sizes [9]. However, this achievement has not been without significant challenges as optical limitations in photolithographic processes impose strict geometrical limits. Photolithography is based on the transfer of the pattern from mask to a photosensitive polymeric layer, or photoresist. Chemical treatments allow the removal of the exposed polymer (positive resist) or the un-exposed polymer (negative resist). Subsequently, chemical or plasma etching is performed in order to pattern the underlying silicon substrate. An alternative technique for silicon patterning is by Focused Ion Beam (FIB) milling [10,11]. In this case a focused beam of ions (typically Ga⁺) is used for material ablation. Although achievable resolution is very high (in the order of nanometers), FIB milling is a time-consuming technique and the patterned area is in the order of hundreds of square microns. Molds of composite (silicon-polymer) or polymeric materials can also be fabricated by means of additive manufacturing techniques like 3D printing [12]. 2-photon polymerization systems allow to reach high resolutions (sub-100 nm) in relatively large printing areas. However, this technique has its set of issues as well: polymeric structures can deform if subjected to high temperature or pressure, and adhesion between the printed structure and the substrate can be problematic [13].

Despite the fact that the aforementioned mold-replication techniques are considered promising as high-throughput patterning methods, there is still a need to improve the mold fabrication process. In particular, the possibilities for creating highly precise patterns at the nanometer scale with large areas by means of a low cost, fast and efficient process are still under development.

Alternative studies propose the development of a bottom-up method based on self-assembly, where small prefabricated building blocks,

such as nanoparticles, are allowed to organize into final, reversible, structures. Herein inspiration is often drawn from nature, where these processes occur on an ubiquitous scale [14]. Small particles suspended in a solution, so called colloidal particles or colloids, can be used as building blocks within the self-assembly process, by setting the local environmental conditions such that they form into predetermined colloidal surface [15].

As colloidal lithography [16], a collection of methods based on the use of colloidal structures for pattern replication, is a relatively new research field, the goal of this review is to explore the already available techniques for the creation of self-assembled colloidal crystals. Initially, an overview of the properties of colloidal particles is presented. Then, the most relevant self-assembly techniques are described, focusing on the realization of 2D crystal at a liquid/solid interface. This is the most suitable self-assembly arrangement that can be used for replication where an ordered 2D pattern is transferred onto a flat polymeric substrate. Finally, an overview of developed processes where these colloidal structures are used for pattern replication is presented.

2. Colloidal particles and interactions

Colloidal particles are an intensively studied material as an option for the building blocks required for self-assembly [17–19]. Ranging in size from a few nanometers up to a single micron, their small size renders them subject to Brownian motion. However, this also makes them readily available to be suspended in a variety of liquids, forming so-called colloidal suspensions. Their most attractive feature is their tendency to form crystalline organizations, which allows them to be used as intermediate building blocks for larger and more complex structures [20].

2.1. Colloidal particles

Several techniques and protocols have been developed for the synthesis of colloidal particles. Depending on the used material (e.g. gold, silica, polystyrene), colloidal particles can be synthesized by suspension-, emulsion-, dispersion-, and precipitation-based polymerization methods. In general, factors that affect the size and polydispersity of particles are pH value, the concentration of catalyst, the composition of reagents, the types of solvents, and the reaction temperature. Several reviews offer a complete overview of colloidal particles synthesis and characterization [21–24].

It is important to mention that functionalizing the surface of a colloidal particle may also alter its surface chemistry [25]. The main

usage for colloidal surface functionalization is to prevent agglomeration, with common functional groups being hydroxyl (—OH) and carboxyl (—COOH) chemical moieties. Particles can also be encapsulated by a metal or oxide shell to allow for further functionalization [26].

An interesting development is the synthesis and use of Janus particles [27,28]. These are particles which have been synthesized, functionalized or altered such that they exhibit a high degree of asymmetry, in terms of morphology and/or chemical interaction. This is most often achieved by combining two materials with distinct chemical properties. Due to the inherent non-homogeneity of these particles as self-assembly building-blocks, a larger variety of colloidal structures can be created.

Typically, functionalization is performed uniformly around the surface of the particles. However, so-called *patchy particles* can also be obtained by functionalizing only a part of the surface. Pawar and Kretzschmar [29] developed a technique called Glancing Angle Deposition (GLAD), in order to selectively functionalize the outer shell of particles, wherein a metal is deposited onto a preformed colloidal monolayer which is tilted under an angle. As the deposition is dependent on line-of-sight, the particles are selectively coated [30].

2.2. Interactions between colloidal particles

The behavior between colloidal particles is governed by a large number of interactions, and the colloidal crystal formation and stability result from a balance between the different forces. A brief overview of the most important interactions is given here, both between particles surrounding environment [31–35].

2.2.1. van der Waals interaction (vdW) [36,37]

vdW interactions result from the interaction between the individual constituent of the particles. It is possible to exploit this energy to drive self-assembly, however this works most effectively only for small, nanosized, particles. vdW interactions rely on short range forces that are overcome by other forces for surface separations exceeding 10 nm. As interaction distances increase to larger ranges, the influence of vdW interactions falls off rapidly.

2.2.2. Electrostatic interaction [38,39]

Electrostatic interaction occurs due to particle surface charges and can be either attractive or repulsive. When particles are suspended in a liquid, the electric double layer effect comes into play, creating an electric field and therefore yielding a slight repulsion between two or more particles. The decay of this effect's influence is usually expressed in terms of the Debye screening length or screening effect; it depends on the electrolyte concentration, pH and particle concentration. It is important to mention that electrokinetic phenomena due to the movement of charged particles can be very influential during colloidal crystal formation.

2.2.3. Steric effect [40]

Colloidal particles in highly concentrated media are subject to steric effects, where the presence of other particles in the liquid physically blocks further ordering or material deformation. One key steric effect is depletion interaction, which occurs when particles suspended in a solution approach each other and a solute molecule no longer fits in between them. The particles are then pushed together, as the surrounding molecules of the liquid exert an osmotic pressure. This effect is especially prevalent in macromolecular solutions, such as liquid crystals and polymers.

2.2.4. Capillary forces [41]

Attractive capillary forces originate due to the formation of liquid bridges, typically observed in meniscus effects, forming between particles due to surface tension. Their behavior can be modelled by Laplace Pressure.

A large number of additional forces can also play a role in colloidal self-assembly, including structural forces, fluctuation wave forces, bridging interaction and solvation forces [31].

2.3. DLVO theory

The Derjaguin–Landau–Verwey–Overbeek (DLVO) theory [42,43] is commonly used to determine the stability of colloidal suspensions. It corresponds to the balance between van der Waals attraction and electrostatic double layer repulsion, the total energy of which can be approximately described as the total interaction between two circular plates, in Derjaguin's expression, by summing the DLVO interaction energy per unit area over the entire domain:

$$U_{DLVO} = f(a) \int_D^{\infty} (U_{EDL}^A(h) + U_{vdW}^A(h)) dh$$

where $U_{EDL}^A(h)$ is the electric double layer energy, $U_{vdW}^A(h)$ is the van der Waals energy, D is the minimum particle-surface distance and $f(a)$ is a geometrical correction factor dependent on the particle radius a , which approaches zero as h approaches ∞ . Within the DLVO theory the particle surface is regarded as continuous but can also be constructed as a summation of several discretized infinite parallel plane models. This approach allows the numerical computations of particle-particle and particle-surface interactions. Extended models also take into account surface roughness [42,44].

Although the DLVO theory is a powerful tool, it does have its limitations, namely because the electrostatic decay, due to screening, is expressed in terms of the linearized form of the Poisson-Boltzmann equation. Secondly, transient boundary conditions such as the change in electrostatic potential or charge density on the surface are not taken into account; although not relevant for long range interactions, this is crucial for modelling short range interaction more exactly. For a more extensive overview of the influential forms of interaction energy the reader is referred to the review by Bishop and co-workers [33].

3. Self-assembly techniques

Self-assembly is a method wherein a structure is spontaneously assembled without the influence of external forces [14], excluding manipulation by robots and direct manipulation of the building blocks. Due to this inherent autonomy this principle is seen as a promising step in fabrication of nanostructures [45,46]: structures would be able to be assembled with a high degree of precision, due to the minimization of energy leading to the final state of assembly. Potentially, this could lead to fewer defects and more stable structures [47].

A distinction must be made between direct and indirect self-assembly. In the former a global minimum energy is reached in a purely self-governing fashion, while in the latter the system is designed in such a way that the building blocks end up in a local energy minimum. Therefore, directed self-assembly requires a high level of control but allows for a larger variety of structures [20]. Many approaches have been used for achieving directed self-assembly such as, but not limited to: external fields [20], evaporation [48], surface tension [49] and interface interaction [50].

This review is focused on the realization of colloidal crystals suitable to be used as molds in replication processes for polymer substrate patterning. Several classification criteria for colloidal self-assembly have been proposed [15,51]. In this review, the self-assembly methods are organized based on the type of dominant force that is mainly responsible for the particle assembly, in order to provide the reader with a comprehensive comparison of the various approaches that can be used to achieve a controlled self-assembly of colloidal crystals. We aim, by this classification, to offer a list of possibilities that researchers in the field can utilize, best suited for integration into a wider but specific manufacturing process flow.

We have identified four main categories:

- Physical: self-assembly process dominated by shear forces, adhesion and surface structuring;
- Fluidic: self-assembly process dominated by capillary forces, evaporation, surface tension;
- External Fields: self-assembly process dominated by electric and magnetic fields;
- Chemical: self-assembly process dominated by chemical interaction, changing the surface charge or creating binding sites.

A graphical overview of all treated methods is given in Fig. 1.

Furthermore, the focus of this review is on 2D crystals without considering multi-layer self-assembly and taking into account only the type of forces which dominate the self-assembly process. Other parameters such as the realization of close-packed layer or the type of particle (dimension, anisotropy [52] or material) are not considered as criteria of classification.

3.1. Colloidal crystals

Crystallization is usually described as the process of organization of small groups of molecules into larger, well-ordered structures called phases. The process of crystal formation is largely driven by the nucleation of these groups of molecules. Different crystalline structures can exist within the final compound, also known as polymorphism [53].

As colloidal particles can be seen as an analogue to simple atomic liquids and solids, they too can form crystalline structures, called colloidal crystals. Spherical colloids have been used predominately in the past, as they have only a single degree of ordering [54]. The most common crystal forms for such particles are hexagonally close packed (*hcp*) and cubic close packed crystal (*ccp*) structures [55]. The formation of these can be described by looking at the thermodynamic minima or entropic differences between the two crystal lattices. In terms of minimum Gibbs energy, the *ccp* structure was determined to be slightly more stable than the *hcp* one. However, both share a similar two-dimensional close packed structure, with the difference between the two being the stacking within the third dimension [56]. To express the total amount of space occupied by particles versus available space, the packing density is used. For close packed structures the packing density is around 90.7%, while for a square packed lattice it is 79% [57].

The usage of colloidal particles as a bottom-up assembly technique has been intensively studied over the years [14] and, as such, a wide variety of methods exist that allow the creation of either monolayer or multilayer colloidal crystals, mostly in *ccp* or *hcp* crystalline form due to their thermodynamically minimal states [58].

The realization of a patterned mold for replication into polymers needs a high control over the morphology of the self-assembled particles. Potentially, precisely controlled structures could be achieved by directing the self-assembly of the colloids not into global minima, but into different local and stable states, so that novel structures could be developed.

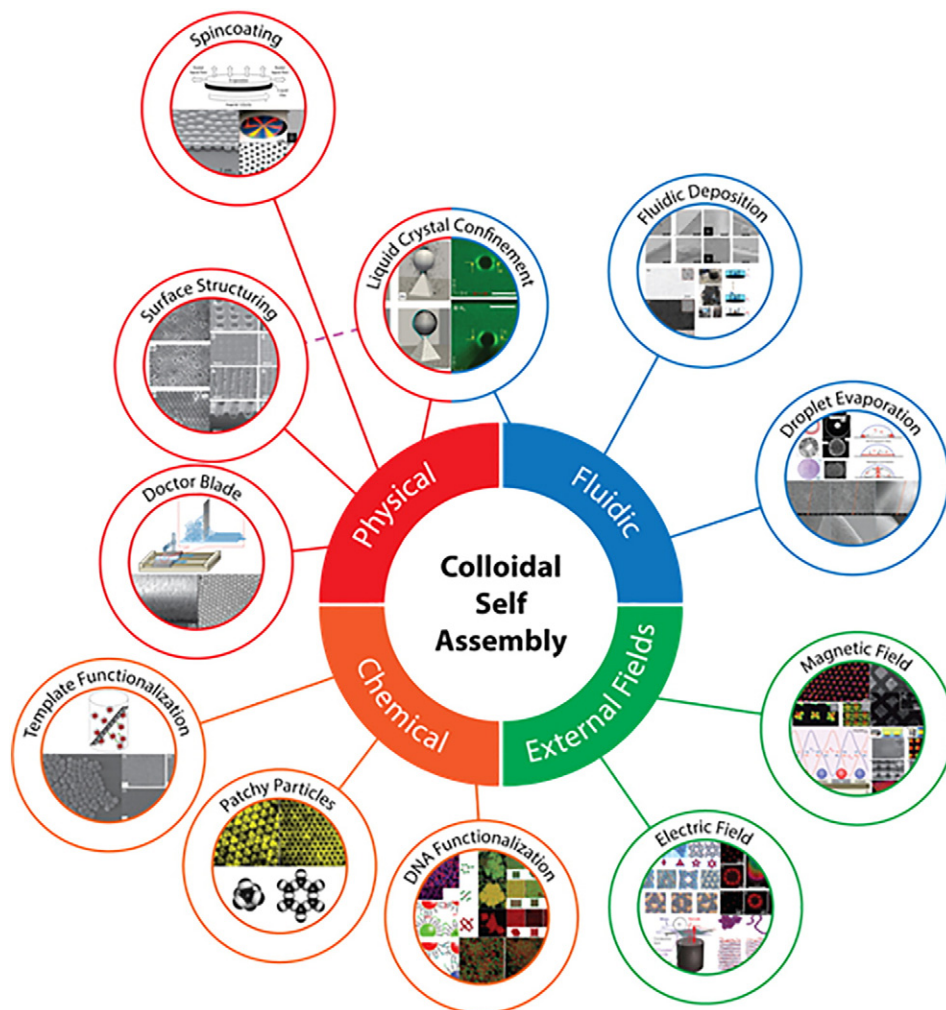


Fig. 1. Scheme of colloidal self-assembly techniques. Each of the 4 domain (physical, fluidics...) indicate the origin of the main force which drives the process.

3.2. Fluidic

For fluidic methods the governing forces are resultant from the interactions between the particles and the solvent. This means that the crystals are a product resulting from surface tension, evaporation, capillary forces or a combination of those. These methods are already quite well developed because of their simplicity and use with different materials. Still, they do pose some unique challenges for future research.

3.2.1. Fluidic deposition

The formation of monolayers has long been well understood as these can be simply synthesized through a device called the Langmuir-Blodgett [59]. The working principle, shown in Fig. 2, is straightforward and commonly used with surfactants, such as oil. However, it can be applied to colloidal materials as well, as long as they allow the formation of a monolayer at an interface. When a colloidal suspension is dispersed onto a surface, the colloids spread as far as possible, forming a spaced monolayer on the surface. The film is then compressed through a barrier which reduces the available surface area, resulting in an increased surface tension. When a substrate is then 'scooped' through this compressed film, the lower surface tension provided by the substrate will cause the colloids to transfer from the interface.

To understand the effect of surface chemistry of the substrate on colloidal crystal formation, Reculosa and co-workers [60] tested several hydrophobic substrates by trying to create colloidal crystals using variously functionalized silica particles. However, none of the silica particles were able to attach onto the hydrophobic surface, which implies that the interaction between trough liquid (sub-phase) and substrate dominates the interaction between particles and substrate. Therefore, the hydrophilicity of the substrate plays a fundamental role during self-assembly with a Langmuir-Blodgett method. The technique has its limits in terms of particle size and functionalization. Moreover, crystal damage can easily occur in Langmuir based processes due to capillary forces. When a substrate is scooped in or the water level is lowered it can result in particles adhering to the walls, which causes stresses within the crystal.

A method developed by Lotito and Zambelli [61] allows the creation of highly ordered colloidal crystals, with little defect. In this method, a monolayer was allowed to form on the air-water interface within a floating rubber ring. As the water level was lowered the monolayer gently transferred onto a substrate which was placed under water. Fig. 3 shows images of this setup (a–d) and the working principle (i–iii). To form a monolayer, 200 nm polystyrene (PS) spheres were deposited onto a slanted substrate which, due to the angle, caused the dispersion to transfer onto the interface. The angle of the substrate proved to have no influence on the transfer. A rubber ring, constrained by three rigid pillars, was used to contain the monolayer. To insure a clean transfer the tank was slowly drained at a controllable rate between 0.25 and 5.5 ml s⁻¹, in order to prevent the occurrence of

turbulence, which would have resulted in destructive shear forces. In this fashion, square samples up to about 6.45 cm² and circular samples with a diameter of up to 10.15 cm were fabricated. By combining particles of two different sizes so called binary colloidal crystals were also produced, in which smaller spheres filled the interstices of the larger ones. However, these crystals showed to be more defect prone than their non-binary counterparts. Images of both singular and binary crystals are shown in Fig. 3A and B respectively.

Hatton and co-workers [62] developed a method in which they could significantly reduce the formation of cracks and other defects present in large scale colloidal self-assembly due to strong capillary forces. Poly(methyl methacrylate) (PMMA) particles, with a diameter between 250 nm and 400 nm, were synthesized and suspended in deionized water at approximately 0.125% volume. A sol-gel precursor, tetraethoxysilane (TEOS), was added into the suspension at a percentage of approximately 0.75 of the volume of the colloidal solution. Then, a substrate was put into the suspension, and a meniscus which formed due to surface tension caused the transfer of the particles. By increasing the temperature to 65 °C, until full evaporation of the suspension after 1 to 2 days, the depositing meniscus was forced to slowly travel down the substrate during evaporation. The addition of the silica gel caused the particles to stick together better, forming temporary "glue-like" connections. An additional benefit of this method is that the formation of the crystal proved to be independent of the shape or curvature of the substrate.

3.2.2. Droplet evaporation

The droplet evaporation method is based on the drying of a droplet of suspended particles. Three main flows regulate the self-assembly process: a radial evaporative flow dependent on the flux and the density of the fluid, a recirculating 'Marangoni' flow caused by surface tension gradients and a flow caused by the DLVO adhesion force, introduced earlier [63].

Evaporating droplets of colloidal suspension is a popular approach to self-assembly due to its simplicity and speed. However, it is a method which remains difficult to control as flows within the droplets caused by rapid evaporation often lead to non-uniform patterned surfaces. Large numbers of particles end up either near the edge or in the center, a phenomenon popularly known as the coffee stain effect [64].

An analysis performed by Bhardwaj and co-workers [65] showed that this effect can be overcome by altering the pH value of the suspension. In their experiments, titanium dioxide particles with a diameter of 25 nm were suspended in water and dried in air. By adding either hydrochloric acid or sodium hydroxide the pH value of the suspension was lowered or increased, respectively. The effect of this process is that the DLVO force is either attractive, at low pH values, or repulsive, at high pH values. This causes particles to form in a well-defined ring at high pH values, while depositing themselves over a uniform surface at low pH values. The final location of the particle is strongly dependent

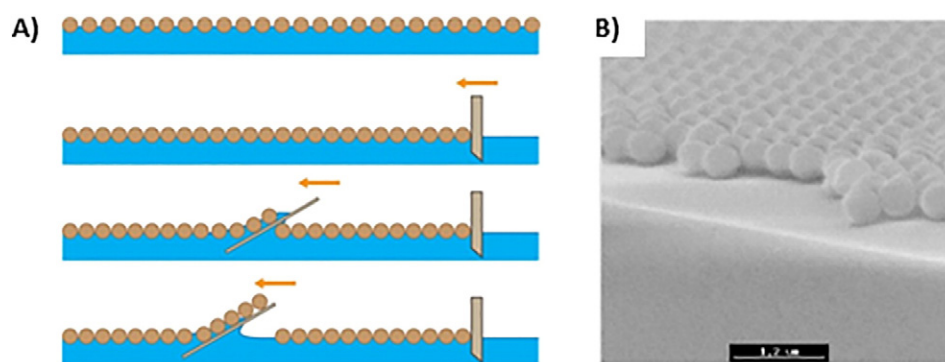


Fig. 2. Fluidic deposition: Langmuir-Blodgett method. A) Schematic drawing of the method. B) SEM images of a monolayer of colloidal crystals. Adapted with permission from [60]. Copyright 2003 American Chemical Society.

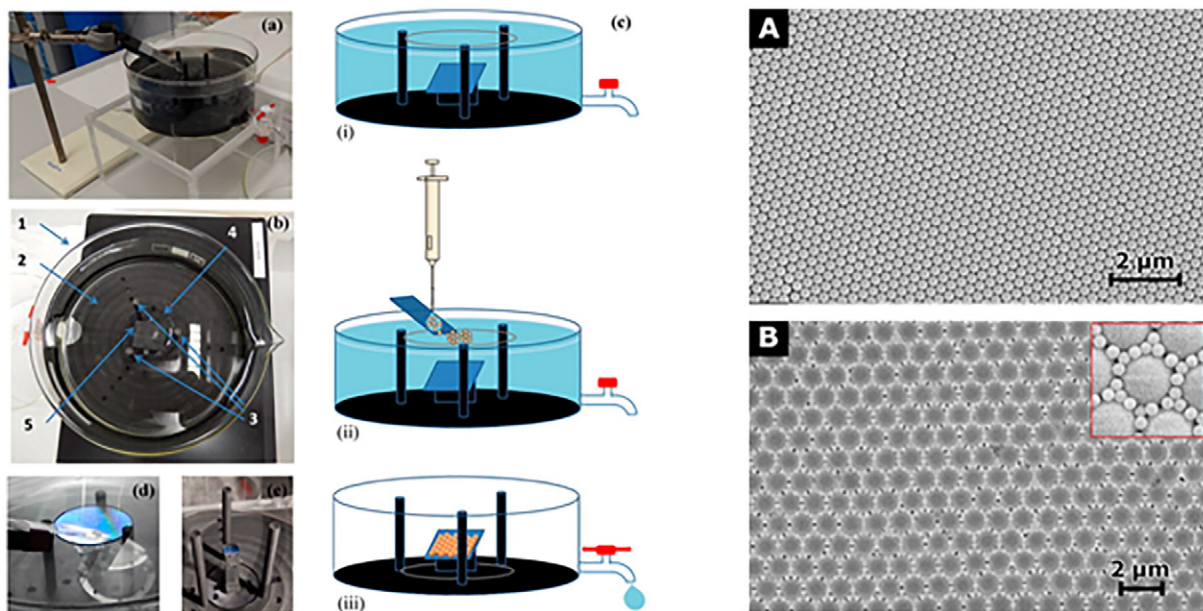


Fig. 3. Fluidic deposition: water discharge method. (a)–(d) Pictures of the setup; (i)–(iii) schematic drawing of the working principle: a colloidal suspension is dispensed on the air–liquid interface, after which the tank is drained. SEM images of (A) hexagonally close packed crystals and (B) binary crystals, formed from a suspension with two distinct particle sizes. Adapted with permission from [61]. Copyright 2016 American Chemical Society.

on the repulsive or attractive nature of the DLVO force. The relationship between the pH value and final deposition location is shown in Fig. 4.

Droplets of colloidal suspension can also be deposited by an ink-jet method, as demonstrated by Ko and co-workers [66]. They evaluated the effect of the contact angle during the self-assembly process of silica particles. Depositing on hydrophilic silica substrates, treated with octadecyltrichlorosilane (OTS) surfactant, the final colloidal crystal was hemispherical in nature and close packed, with a packing factor of up to 77%. For the non-treated silica substrate the packing density could be as low as 24%, with flat disk-like randomly structured aggregates and a well-ordered monolayer at the edge. Copper substrates

also produced hemispherical structures, but with a lower packing density than the hydrophobic silica one. The formation of the resulting structures can be found by looking at the mechanics of evaporation. For flat droplets, with a low contact angle, the evaporation mainly takes place at the edge, so that new particles are drawn by capillary forces from the thicker section of the droplet which pin on the contact edge. However, for more spherical droplets on hydrophobic surfaces, the degree of evaporation is uniform over the surface, resulting in a close packed aggregate.

As illustrated, the coffee stain effect is a product of a too high contact angle between the colloidal droplet and the substrate. Majumder and

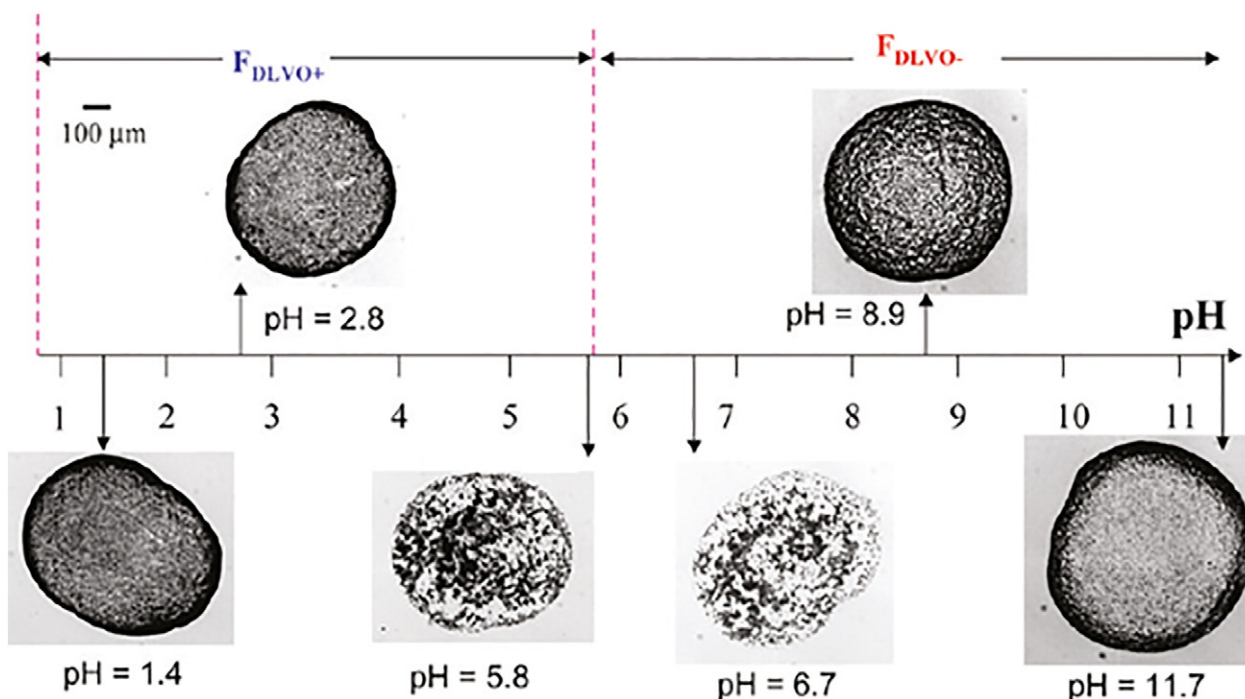


Fig. 4. Droplet evaporation. Difference in final particle deposition under the influence of the pH value. Adapted with permission from [65]. Copyright 2010 American Chemical Society.

co-workers [67] established a simple method by using an alcohol saturated atmosphere to increase the contact angle and reduce the evaporation rate. This phenomenon was then experimentally exploited by dispensing a suspension of iron nanoparticles on a hydrophilic silica substrate. Evaporating the nanoparticle solution in an ethanol atmosphere resulted in the formation of a sparse deposition over the entire surface, showing that the technique could be used to create uniform nanoparticle depositions on functionalized silica.

3.3. Physical

Methods described as physical are considered to rely on self-assembly where shear forces, adhesion and surface structuring are the main driving forces.

These kinds of self-assembly methods generally have a high throughput and make use of well-established manufacturing techniques. Therefore, this makes them foremost candidates for large-scale industrial application.

3.3.1. Spin-coating

Spin-coating is widely used in the semiconductor industry to create uniform layers of photoresist onto wafers for lithographical patterning. After a solution is dispersed onto a substrate in a spin-coater, a rapid acceleration is produced to cause centrifugal forces. This will cause mass to be ejected and results in the topographical “thinning” of the liquid film, with the minimal thickness of this process being dependent on the balance between adhesive and shear forces. Ultra-thin films down to several tens of nanometers can be reached, depending on the used solution [68]. Fig. 5 shows a schematic drawing of the spin coating process.

A spin-coating technique was developed by Jiang and co-workers [69] that allows for the rapid production of colloidal crystals out of silica particles (diameter from 2 μm to 100 nm) suspended into the viscous, non-evaporating and non-volatile monomer ethoxylated trimethylolpropane triacrylate (ETPTA), to which a photoinitiator (Darocur 1173) was added to enable UV curing. Substrates on which they tested their method included silicon wafers, glass slides, lithium niobate wafers and PMMA plates. To achieve thin films, two spin-coating steps were performed. First the wafer was spin-coated for half a minute at 200 rpm until a six armed monochromatic diffraction star appeared, due to the presence of a *hcp* crystal lattice. In the second step, the spin speed was accelerated at 2000 rpm/s to a final spin speed, which varied depending on the desired film thickness. After spin-coating, the wafer was transferred to a vacuum chamber where the ETPTA was polymerized by UV light. The thicker film that forms at the edge of the substrate during spin-coating, due to the higher surface tension, was removed with acetone. Oxygen plasma etching was used to liberate the silica

particles from the polymer matrix. After the removal of the polymer matrix, the final colloidal crystals was observed, through SEM Imaging, to have a *hcp* structure. However, the top most layer was found to deviate from the expected close packed *hcp*, with a larger centre-to-centre distance of 1.41D, where D is the particle diameter. The formation of the *hcp* structure can be explained due to the following observations: shear plays a dominant role in the crystallization, causing layers of the crystal to slide over each other during the spin-coating. While electrostatic repulsion has little effect on the formation, as adding salts to the dispersions had negligible effects. Lastly, vertical packing is dependent on a pressure gradient normal to the spun film, with the pressure being highest at the substrate. The researchers believed that the photo-polymerization step also plays a role in the final crystalline structure, as the ETPTA film shrunk towards the substrate by 4% in volume during curing.

Using the previously described method proved to be very difficult for creating colloidal monolayers, as experimental reproduction was poor. Discontinuous islands of disordered colloids were found with surface areas as large as 1 mm^2 . Therefore, a second study [70] was performed aimed towards producing monolayers. One major change was the much slower increase in the spin speed, with the initial spin speed set to 200 rpm the speed was increased in five steps up to 8000 rpm, and the spin speeds being held constant for several minutes in between the steps. Using this stepping method, monolayer polycrystalline colloidal crystals were found with a domain size smaller than for the case of multilayered crystals. However, a centre to centre distance of 1.417 was seen, equal to that found for the particles on top of the multilayered colloidal crystals. Over fifty samples were prepared and all resulted in monolayer crystals.

The technique is simple and fast, with the sample preparation time around half an hour. However, the self-assembled monolayers remain quite fragile and any further processing should be done with the utmost care [70]. Even though colloidal crystal formation by spin-coating is a promising technique, it is limited by defects, many of which are the result of improperly tuned parameters, such as spinning speed and acceleration.

As most colloidal suspension are commercially provided in evaporating solvents, Toolan and co-workers [71] sought to better understand the balance between shear forces, generated by the spin-coating, and the attractive capillary forces caused by evaporation. As adhesive forces are dominated by convective particle flux, capillary forces will interfere with the growth of the crystal. To study these interactions, they observed the spin-coating of the crystals as the suspension was still wet. This was performed by spinning dispersions at 1250 rpm and observing the samples via stroboscopic microscopy, resulting in a steady image of the phase separation as the same area is sequentially imaged.

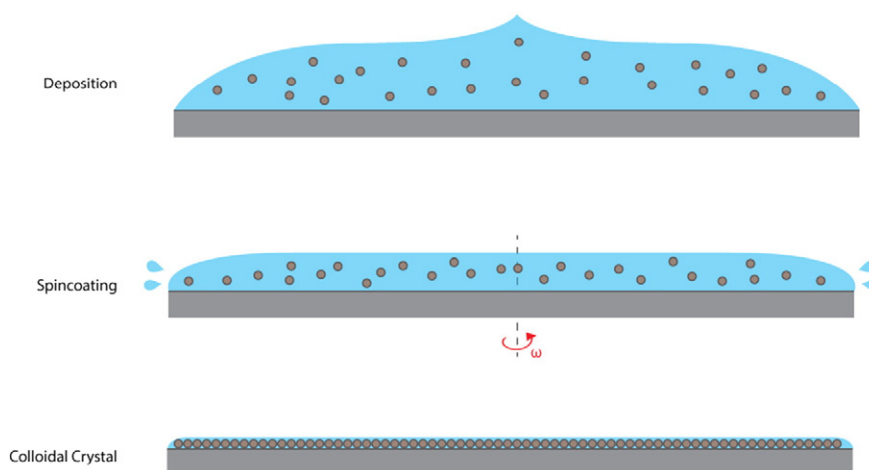


Fig. 5. Spin-coating. Schematic drawing of process.

In their experiments, PS particles were dispersed in both water and ethanol in different concentrations. With a low mass fraction, the particles initially spread out in a loose and random order due to shear thinning, where they can be mainly seen to be moving in clusters. A few seconds later evaporative thinning dominates the shear thinning, which causes a radial outflow away from the center. Ordering in the crystal takes place due to capillary effects, where wetting fronts push the particles away. However, if the shear forces are too high gaps can appear in the crystal as clusters detach from each other. After 16 s the morphology becomes fixed, however, any gaps that formed earlier will grow in size as they fill with fluids. A high mass fraction results in close packed structures forming earlier and small multilayer crystalline regions being separated by defects, opposed to incomplete monolayers found at lower mass fractions. Evaporation of the dispersant thus showed to play a dominant role. For the ethanol dispersions, no radial outflow was observed and a densely packed monolayer forms after just 1.5 s, on top of which a layer of disordered particles forms due to the rapid evaporation.

By applying statistical experimental design Cheng and co-workers [72] managed to optimize and identify the most important parameters for producing colloidal monolayers. Through their optimization of a two-step spin-coating process they produced defect free surface areas larger than $3000 \mu\text{m}^2$. They identified that the relative humidity of the environment plays a large role in the final quality of the colloidal crystal, which was explained to be due to the mechanisms behind the formation of colloidal monolayers of silica particles. As the water film is less thick than the diameter of the silica particles being spun, capillary forces between the particles cause them to be pulled into a close packing configuration. When the particles travel, unoccupied sites cause water to evaporate and lead to convective flow which pulls in new particles, causing crystal growth. However, if the humidity is too high there will be very little evaporation and longer spinning speed times are necessary. Diffusion of particles can also occur when there is too much water, which leads to defects. Optimal packing was found under the condition of a relative humidity of 23% and an initial spin speed of

1000 rpm. In these conditions spinning the crystal for 10 or 30 s resulted in no difference in quality, while high spin speeds resulted in a decrease in crystal quality as particles were ejected.

3.3.2. Surface structuring and liquid crystal confinement

By modifying the surface of a substrate the conditions can be tuned in order to precisely steer particles into global minima. An example of this is an approach based on the modification of a substrate by a holographic technique, which was applied for colloidal patterning by Ye and co-workers [73]. A thin polymer film, containing azobenzene, was treated so that a sinusoidal topographical pattern was formed in the film. Subsequently, the film was deposited vertically into a vial containing an aqueous suspension of PS spheres and was heated to 55°C . Slow evaporation, as described in the section on deposition techniques, lead to self-assembly by a meniscus effect. After the main body of liquid had evaporated from the surface, small amounts were still trapped in pockets which evaporated much slower, resulting in resulting capillary forces which drew any particles close by into the pockets. Fig. 6A shows a schematic drawing of the working principle of this reordering step. Particle diameters between 300 nm and 800 nm were used and the grid spacing was altered so that different crystalline structures could be created, with a ratio between the two defined as $x = d/p$, where d is the particle diameter and p the period of the wave. In Fig. 6B all crystal lattices produced by this method can be seen that were found when varying x .

Trapping particles can also be performed on particles smaller than 100 nm, as shown by Xia and co-workers [74]. A substrate was patterned by photolithography such that physical grooves and holes, with a line thickness less than 200 nm, were etched into silicon such that they could trap particles during spin-coating. Dispersions of 1% weight fraction were spin-coated onto the patterned substrate, trapping silica spheres, of around 80 nm in size and smaller, into the features. The colloids were initially suspended in water, but it was also shown that altering the pH value by either adding hydrochloric acid (HCl) or an

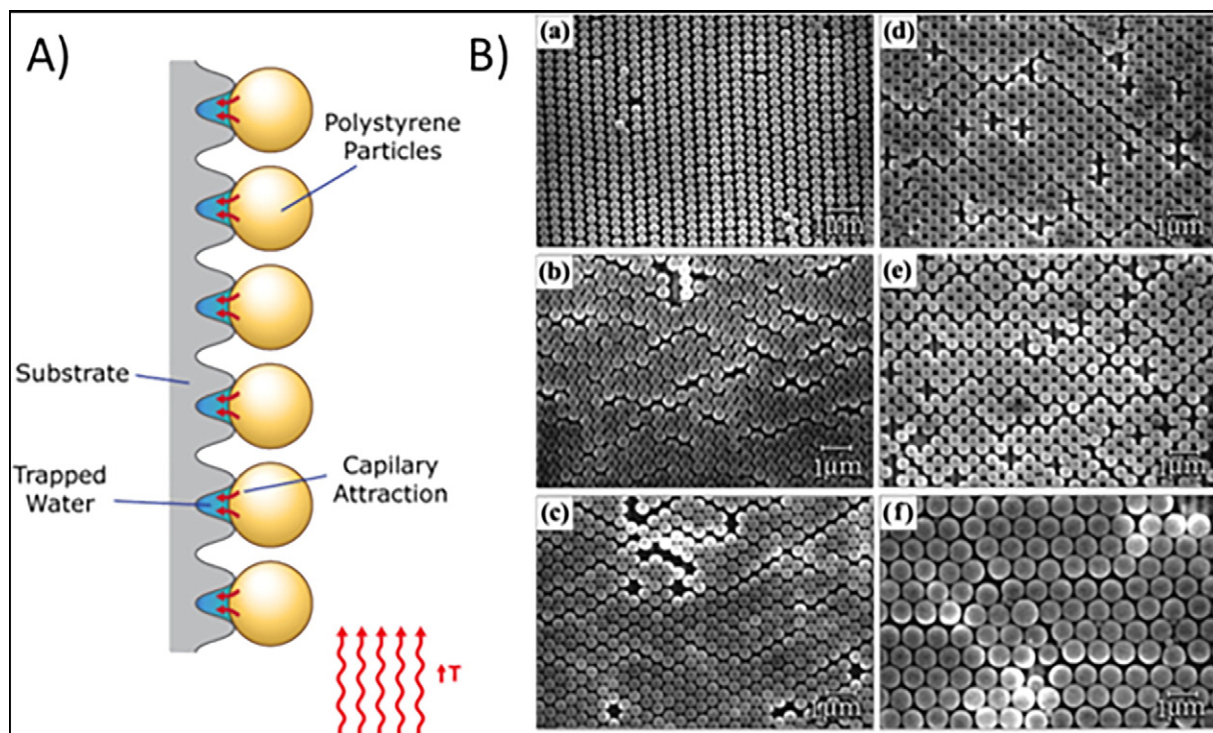


Fig. 6. Surface structuring. A) Schematic drawing of the modified substrate and the capillary attraction exerted on the colloidal particles under heat induced drying. B) SEM images of colloidal patterns resulting from template driven self-assembly. (a) Stripe structure, ($x = 0.74$). (b) 2D centered-rectangular lattice, ($x = 1.05$). (c) 2D hexagonally close packed lattice, ($x = 1.15$). (d) 2D centered-rectangular lattice, ($x = 1.33$). (e) 2D centered-rectangular lattice, ($x = 1.4$). (f) 2D hexagonal lattice, ($x = 2.0$). Reprinted from [73] with the permission of AIP.

ammonia solution (NH₄OH) altered the final position. Increasing pH values above 7 resulted in negatively charged silica spheres sticking to the non-patterned surface more easily.

Trapping techniques were shown to effectively work on even smaller scales as well by Asbahi and co-workers [75]. Substrates with nanostructures were produced including trenches, posts, rectangular holes and comb-like structures, which were then dipped into the colloidal suspension (particles diameter of 12 nm) after which they were slowly pulled out (0.1 to 0.5 mm/min). A thin film formed on the surfaces that evaporated until a monolayer of particles within the fluid was present, which could not further evaporate due to intensity of the van der Waals attraction. Depending on the fluid, the thickness of this film is around 5 nm to 30 nm: thin enough such that the heat flux through this area can be considered zero, meaning that it will possess the same temperature distribution as the substrate, even when superheated. However, van der Waals attractions also generate what is called a disjoining pressure, which is expressed as $P_d = \frac{A_H}{6\pi\delta^3}$, where δ is the thickness of the non-evaporating film and A_H is the Hamaker constant. This effect causes the particles to be pushed into locations due to a pressure gradient, which for the rectangular shaped cavities happens to be the corners, as was expected.

Statements are made that the film does eventually dry out, even though the evaporation was assumed to be contained by the van der Waals interactions. It is likely that some evaporation not accounted for in the model does occur, as it is based on the Young-Laplace equation which assumes the fluid to be continuous [76,77].

For well-defined structures, it is possible to predict and influence the self-assembly process by minimizing the interaction energy between particles and substrate. Silvestre and co-workers [78] were able to predict and experimentally verify the energy minimization and subsequent interaction of a colloidal particle suspended in a liquid crystal interacting with a similar sized pyramid. They performed a numerical minimization using a finite element method, by taking the total energy between particle and substrate as a composition of the energy of the liquid crystal and the surface potential. For both silica particles, of 3.14 μm , and melamin resin, of 3 μm , they found that the particle, liquid crystal and pyramid system resulted in an energy well at the tip of the pyramid. This was then experimentally verified by grafting a pyramid onto a glass substrate by curing an epoxy in a pyramidal shaped mold. A particle suspended in the liquid crystal 4-pentyl-4-cyanobiphenyl (5CB) was introduced and its interaction with the pyramid was observed. Its position in relation to the pyramid was tracked by a fluorescent imaging technique.

Unfortunately, some of the particles were trapped slightly off the tip, indicating that the predicted energy well was off-center. Surface irregularities of the pyramid, with respect to the model, were the most likely perpetrator. Steric effects were not discussed but might be influential in terms of large scale self-assembly. To quantify the 'stickiness' of the particle, or the tendency for it to stay on top of the pyramid, they introduced a dimensionless anchoring strength, defined as $w = \frac{W Q_b^2 R}{K}$ which gives an indication of how strong the force is that keeps the particle in place. In this expression W is the anchoring strength in pN, Q_b a scalar describing the degree of orientation ordering of the liquid crystal, R the particle radius and K the average Frank elastic constant. The elastic constant describes the average magnitude of the free energy of the liquid crystal in all possible degrees of freedom. A higher dimensionless anchoring strength results in a deeper energy well, ensuring particles are more likely to stay fixed on the top of the pyramid [79,80].

3.3.3. Doctor blade: shear and gravity assisted

A doctor blade is a device commonly used to print highly uniform films in the printing industry and used as well to create ceramic coatings. Where a perpendicular blade closely moves along a substrate, leaving only a thin film of the initially deposited material. Yang and co-workers [81] extended this technique to produce close packed colloidal

crystals. A amount of 1 ml of silica particles suspended in ETPTA, with a 20–50% volume fraction, was deposited on one side of the blade. The blade was then moved with a controlled speed and a thin layer was deposited in a disordered fashion. However, the layers themselves were each closely packed, so that there was only long range ordering in two dimensions. Three particle sizes of 560 nm, 330 nm and 290 nm were used. The disordered structures are a result of the shear force which, for viscous fluids, has a linear profile expressed as $\tau = -\mu \frac{dv}{dh}$, where μ is the viscosity of the suspensions, v the speed of the blade and h the thickness of the film. This results in a shear of unequal magnitude for each layer, which yields a direct limit on the usable particle size, due to the fact that for particles smaller than 200 nm an even more viscous suspension agent is required to order the particles. Although the method is simple it is also very sensitive to dust and debris, which can easily damage the colloidal crystals as seen clearly in the SEM imaging process.

3.4. External field

In this section several methods are outlined in which external fields, magnetic or electric, play a dominant role in the final structure of the colloidal crystal. Since these fields are generally well understood they can offer a large degree of control on the final structures.

3.4.1. Electric field

Self-assembly with electric fields on polystyrene ellipsoids was performed by Crassous and co-workers [82]. Spherical polystyrene spheres were embedded into a Poly(vinyl acetate) (PVA) thin film and then stretched at different plastic deformation rates, resulting in ellipsoids which varied in aspect ratio (oblate versus prolate radius). Particles with the same aspect ratio were then suspended together with a composite microgel in water at a 1% weight fraction. Dispersions were then placed between glass slides separated at 120 μm coated with indium tin oxide (ITO), to block any passage of the electric field, except through the uncoated part. A uniform field formed between the slides alternating at 160 kHz was applied, to prevent particles from being attracted to the electrodes. Without any applied field, the particles drifted around inside the suspension fully subject to Brownian motion. By overcoming the thermal energy of a field of at least 25 kV m^{-1} the particles align in its direction. After orientation along the field, the particles form long string-like sheets due to electrostatic interactions, after which they close themselves into tubular structures. The coupling parameter $\Gamma = \frac{q^2}{8\pi\epsilon_m R k_B T}$ determines the final shape of the structure, where q is the charge of the PS particle, ϵ_m the permittivity of the medium and R the oblate radius of the ellipsoid. Only ϵ_m can readily be adjusted and as such influence Γ . If Γ has a value of 9.8 the sheet like and subsequently tube like structures are achieved; lower values only result in close packed aggregates. After roughly half a minute of being subjected to the field, tubes were formed, however not all particles participated equally. Turning off the electric field resulted in the structures disassembling and, again, were seen to drift randomly.

While the previous method is a typical showcase of the power of self-assembly, the final result is unstable and highly subjected to thermal influence, with the deformation of the particles influencing the final structures. However, particles don't have to be altered or functionalized in any way to be able to be influenced by an electric field, which was shown by Wu and co-workers [83]. By using the right concentration of salt and an oscillating alternating electric field, the interactions between particles can be carefully tuned. Polystyrene particles were synthesized and suspended in deionized water. Slides coated with ITO were then negatively charged such that a colloidal suspension floated in between the two slides, which were kept separated at a set distance by a non-conducting strut. By varying the salt concentration, formations of molecular like structures appear, which occurs as the forces that usually balance the dispersion are distorted. Three main particle interactions were identified by the researchers: dipolar interaction,

dielectrophoretic attraction and the electrostatic double layer (EDL). Both the dipolar and EDL interaction are repulsive and dependent on the charge of the particle and the surface attached ions, respectively. The dielectrophoretic attraction is a force between particle and substrate that orients the poles of the particle with respect to the electric field. Exploiting these forces, several oligomers were created, including triangular aggregations and pentagonal and hexagonal rings, allowing both the formation of honeycomb and island like lattices. A high salt level and a high switching frequency both resulted in a decreased inter-particle distance, the first being due to the reduction of electrostatic interaction and the second due to the decrease in strength of the field; yet the frequency seemed to impact the formation of oligomer structures the most, which could be reduced by using higher salt concentrations. However, if the salt concentration became too high a close packed monolayer formed. The video footage of the experiments shows that the lattices are transient and stability is low, indicating that the thermal energy is quite influential. Volumetric effects also played a role as too high or too low particle concentrations resulted into either randomly spaced or close packed formations, without clearly defined structures.

Electric fields can also be used to modify the structuring of colloidal crystal found by spin-coating. Such a modified method was developed by Bartlett and co-workers [84], where a non-uniform electric field was added that rotated synchronous to the spinning platform (chuck), influencing the outward flow of the suspension.

3.4.2. Magnetic field

Demirörs and co-workers [85] showed that they could create colloidal arrays from particles that are both attracted (paramagnetic) and repelled (diamagnetic) by using a magnetostatic field [86]. On top of a permanent magnet they placed a grid that focused the magnetic field into a predefined shape, which they called virtual molds. Particles were either trapped or expelled from these molds, depending on their magnetic properties. The grid was fabricated by creating the pattern by photolithography in a substrate, and then using e-beam evaporation to deposit nickel. Subsequently, the nickel grid was lifted off and embedded within PDMS by spin-coating resulting in a flat composite structure. Functionalization by 3-(triethoxysilyl)propylisocyanate (TPI) was performed on the surface to be able to fix amine functionalized particles by covalent attachment. The physical principle behind the interaction of the particles with the field can be explained by the magnetostatic interaction $U_M(\mathbf{r})$, which is expressed by

$$U_M(\mathbf{r}) = -2a^3_0 \frac{\chi_{part} - \chi_{sol}}{\chi_{part} + 2\chi_{sol} + 3} |\mathbf{H}(\mathbf{r})|^2$$

Here the particle location is represented by \mathbf{r} , the magnetic field by \mathbf{H} , particle radius by a and magnetic permeability in free space by μ_0 . As a , the radius of the particles, is expressed cubically, the magnetostatic effect on small particles is very small. Therefore the most important factors are χ_{part} and χ_{sol} , which represent the magnetic susceptibilities of the particles and dispersing medium, respectively. This implies that either a very strong magnet needs to be used, or the magnetic properties of solution and particle need to be tuned. The latter allows for more flexibility, so that both paramagnetic and diamagnetic particles could have the same magnitude of force exerted on them. The research team achieved this by using a solution consisting of an acidic salt ($\text{Ho}(\text{NO}_3)_3$). By using the described method and by using particles of different sizes and magnetic properties, a wide variation of patterns could be created. A few of them are displayed in Fig. 7.

In order to create arrays and for the magnetic field to affect the particles, the spacing of the grid needs to be in the same order of dimension as the particle size. In fact, when particles are larger than the spacing, they will form oligomers. Steric effects do prevent the formation of some structures, however, it can also be exploited to trap large particles into clusters of smaller ones.

By taking advantage of the decay of the magnetic field, bridge-like structures were formed, which form when the gravity and the magnetic force repelling diamagnetic particles balance each other. By applying a second sandwich on top the magnetic field was extended into an hour-glass shape, such that diamagnetic particles could be trapped in-between the fields in an egg-like shape. After removal of the magnet the structures collapsed. To prevent this from happening they can be anchored to the sandwich by carbamide bonds.

3.5. Chemical

By altering the chemistry of a surface or template it is possible to control the interaction of chemical compounds. These kinds of interactions, while large in scale, can also be used to drive the self-assembly of colloidal particles. This section provides an overview of how chemical interactions can be used to control the formation of colloidal crystals.

3.5.1. Template functionalization

An approach used to guide the self-assembly of a large number of particles is the chemical modification of substrates. Li and co-workers [57] came up with a simple technique where they functionalized naturally negatively charged silicon with amine groups to tune the surface charges to be positive. By then introducing silica nanoparticles, of roughly 67 nm in size, they were able to create aggregates of particles

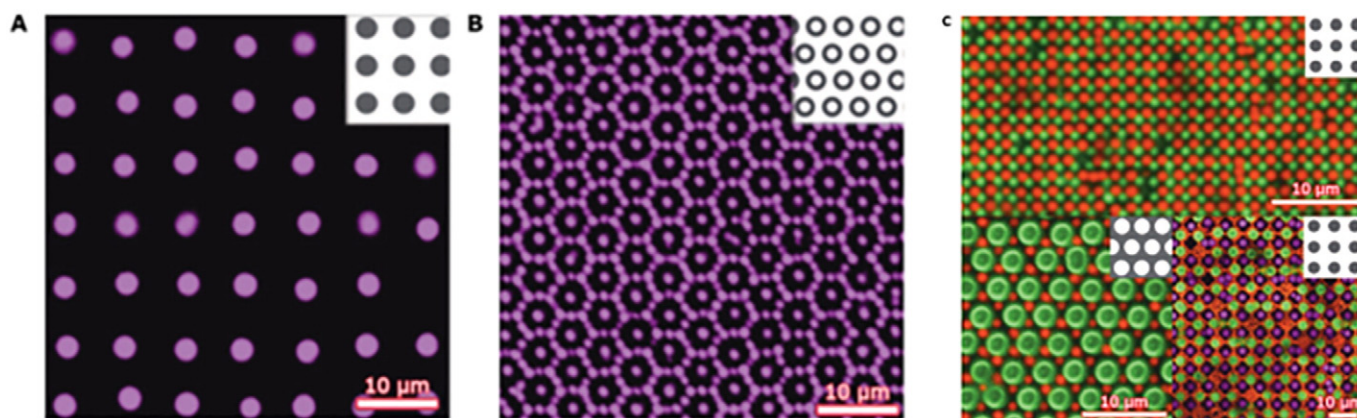


Fig. 7. Magnetic field. By using particles with different magnetic properties and of varying sizes, a myriad of patterns can be created with the same nickel-PDMS grid. (A) Paramagnetic particles 2.85 μm in size assembled at the intersections of the nickel grid. (B) Diamagnetic particles 1.2 μm in size assembled in a hexagonal pattern. (C) Several grids created by combining paramagnetic and non-magnetic particles of different sizes. Adapted by permission from Macmillan Publishers Ltd.: Nature [85], copyright 2013.

on the surface. The amine groups were introduced by exposing an oxygen plasma cleaned substrate to a solution of toluene and 1 mM 3-aminopropyltrimethoxysilane (APTES) for 1.5 h. Hydroxyl moieties on the substrate react with the silane group of the APS, forming a monolayer on the surface. Positively charged tails point away from the monolayer and are therefore able to attract negatively charged silica particles. The change from a positive to negative charge was also confirmed by measuring the zeta-potential, which is a measurement of the total surface charge of a surface. The substrate surface charge was seen to change from -31.4 mV to 16.9 mV after treatment with APS. Unfortunately, the APTES monolayer is very sensitive to any impurities and will degrade if contaminated. A colloidal suspension in a 90% ethanol and 10% water solvent at a weight fraction of 2.04% was found to provide the largest amount of surface coverage, at 63.2% coverage. Either too much (100%) or too little ethanol ($<90\%$) resulted in a lower surface coverage, even though the surface charge was higher for an ethanol suspension, due to the inter-particle effects being too strong. In order to overcome this effect, salt was added to the suspension to decrease the screening length and thus the electrostatic repulsion between particles. At a concentration of 1 mM a total surface coverage of 84.2% was observed. At these concentrations multilayers are also found, but no close packing is observed. They concluded that a large degree of ordering cannot be achieved by electrostatic attraction alone.

3.5.2. Patchy particles

Janus particles can also be exploited to create unique crystals lattices. Due to the asymmetric nature of those particles, the interactions between them are selective and directional, resulting in assembled structures with substantially fewer defects comparing with conventional self-assembly methods [87,88].

Romano and Sciortino showed that particles with two attractive patches symmetrically arranged as polar caps spontaneously assemble in a two-dimensional (2D) Kagome lattice when the patch width is within the range of values that allows for at most two bonds per patch [89].

Chen and co-workers [90] used Janus particles to make 'Kagome' lattices, a 2D assembly of triblock made up of an electrically charged band in-between two hydrophobic polar caps of a proper size. Which was achieved by functionalizing the two poles of spherical particles to be hydrophobic. When the spheres are suspended in deionized water they will try and reduce their wetting surface as much as possible, causing the poles of two particles to approach as close as possible. This was achieved by taking a self-assembled monolayer of sulphate PS particles,

with a diameter of $1\ \mu\text{m}$, and coating them with 2 nm titanium seeding and 25 nm gold layers. To provide functionalization on both poles the particles were picked up by a PDMS stamp and flipped over, exposing the other pole, which was similarly coated. The layer deposition was carried out using the previously described GLAD technique. Using octadecanethiol, a hydrophobic surface was grafted exclusively on the gold surfaces, rendering solely the poles hydrophobic. The particles were then suspended in deionized water. As the electric repulsion between the treated particles is not insignificant, salt (NaCl) was added to the colloidal suspension to reduce the electrostatic repulsion. This way the hydrophobic poles could approach each other close enough to form the Kagome lattice [90], as seen in Fig. 8. To avoid the lattice from sticking to the substrate, and hindering self-assembly, it was negatively charged, so that it electrostatically repelled the lattice. Before the kagome lattice is formed, ring-like structures appear which are metastable. After some time the first kagome lattice forms, but not all particles will take the desired shape. It can take up to 10 h for even 70% of the particles to achieve the desired structure. This could partially be explained due to transient nature of some of the lattice structures, as Brownian motion can cause a shift in shape. Particles are able to form up to four bonds, with two other particles per pole. By stacking multiple kagome lattices, three dimensional octahedron structures were fabricated as well.

A follow up study [91] was performed, where the angle of deposition of the patches was further improved by introducing an etching step. Gold was again deposited from above, however as the deposited layer was thicker on the top of the particles than on the sides a crescent shape deposition was formed. The functionalized particles were then put into the etching solution consisting out of: sodium thiosulfate ($\text{Na}_2\text{S}_2\text{O}_3$), potassium ferrocyanide ($\text{K}_4[\text{Fe}(\text{CN})_6] \cdot 3\text{H}_2\text{O}$) and potassium hydroxide (KOH) solved in water. This slowly etched the crescent away, until the desired spot size was left. The particles were submersed in deionized water and any remaining etching agent was rinsed off. In this fashion, it was possible to create patches at defined angles.

3.5.3. DNA functionalization

By coating colloids with DNA, they can be forced into a structure that diverts from the thermodynamically minimal position commonly found for untreated particles. The advantage of using DNA is that it can be activated and deactivated, effectively allowing the programming of the self-assembly process [92].

Gold nanoparticles were patterned on 2D arrays using hybridization of oligonucleotide functionalized nanoparticles to a preassembled DNA

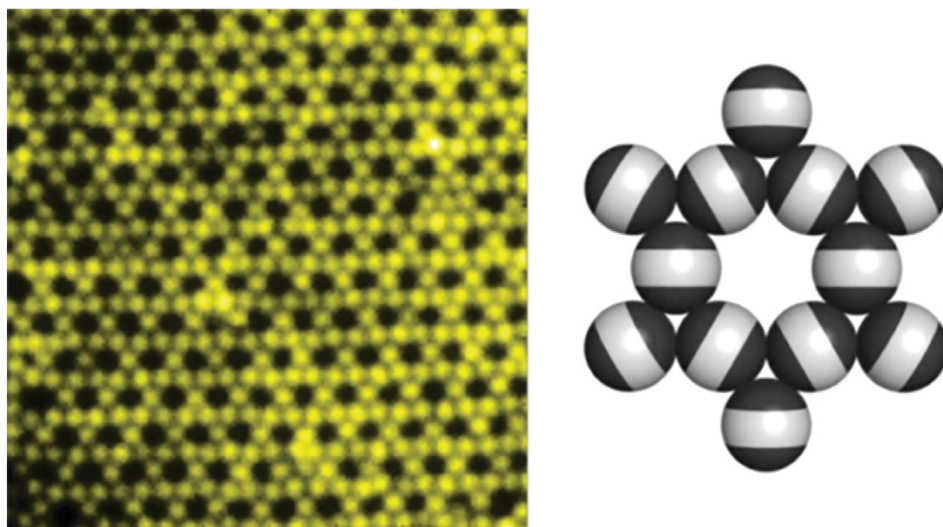


Fig. 8. Patchy particles. Fluorescence image of the kagome structure and a schematic representation of the particle-particle adhesion. Adapted by permission from Macmillan Publishers Ltd.: Nature [90], copyright 2011.

template [93]. In this study, 5 nm gold particles were functionalized with multiple strands of 3'-thiolated DNA (dT15). Then, hybridization between them and protruding complementary (dA15) sequences on one of the template strands was performed leading to the creation of arrays of components in programmable 2D arrangements.

Zeng et al [94], proposed a method for creating a more complex periodic patterns. Gold nanoparticles were attached to strands in two different triangular building blocks, and a well-formed 2D array of alternating 5 nm and 10 nm gold nanoparticles was produced.

However, as DNA is in the size of nanometers, it is difficult to use programmable strands on microparticles. Therefore, Wang and co-workers [95] developed a technique in which they functionalized both silica and polymer particles with a large shell of ssDNA, up to 115,000 strands per particles, for particle diameters of 3.5 μm down to 540 nm. Using 1 μm particles they managed to create a three dimensional colloidal crystal that exhibited a *ccp* structure. Furthermore, by combining particles of different sizes and complementary DNA strands they managed to create crystalline structures resembling those found in metalloids and fullerenes. However, the synthesis of large crystals remains difficult, as DNA has a very specific activation temperature and will not hybridize unless this is reached. Lowering the temperature in turn decreases the amount of diffusion, which leads to the formation of larger crystals. Therefore, the temperatures in the crystallization process have to be properly tuned to take into account both diffusion and DNA activation. Major causes of defects within DNA based techniques are steric effects and the misalignment of local crystals.

4. Nano-patterning with colloidal crystals

As self-assembly methods are simple, cheap and flexible, they are ideal candidates for creating sub-micron features in polymers on large areas [96], in order to avoid the use of complicated techniques and machinery, such as lithographical and other top-down patterning techniques. This section sets out to show polymers structured by patterns created through self-assembly, as well as where potential opportunities are available to further improve on them.

Colloidal crystal can be used as mask for colloidal lithography or as a mold for replication technique (soft lithography and hot embossing). This makes them really versatile for patterning different kind polymers with different techniques. Research on this topic is still in its infancy and we feel that the interest in this approach will grow quickly in the next years.

4.1. Colloidal lithography

Colloidal lithography (CL) is a technique based on the use of a colloidal crystal as a mask for patterning the underlying substrate [97,98]. When a colloidal mask is present, deposition or etching have an effect on the substrate only through the interstices between particles. These interstices can be modified by means of post treatments in order to expand the patterning geometries [99]. Thermal evaporation, sputtering deposition and electrochemical deposition are some examples of techniques that can be used to create patterns on inorganic or organic materials. Several different polymer nanostructures were fabricated by Trujillo and co-workers [100] by combining a colloidal mask (PS nanosphere) with the Initiated Chemical Vapour Deposition Technique (iCVD) [101]. Fig. 9 shows a scheme of the main steps involved in the CL technique. The colloidal mask, which was fabricated out of monodisperse PS nanospheres, acted as a geometrical constraint for the polymer patterning. A p-type silicon wafer was used which was cleaned and hydroxylated using oxygen plasma. Monodisperse PS nanoparticles at 2.5% weight were suspended in water mixed with a surfactant, at a 1:1 ratio, and dispersed in droplets of 2 μl onto the substrate, which was allowed to evaporate for 20 min and further dried in a nitrogen pumped oven. Vinyltrichlorosilane vapor was then allowed to covalently bond to the substrate in a vacuum oven, by removal of the chlorine through hydrolysis. This process left behind a monolayer of vinyl-silane serving as coupling agent for the polymer film. Without this coupling agent the films were found to easily detach when exposed to the cleaning agent used to remove the colloidal mask. With the mask attached to the surface, the polymers were deposited using the iCVD technique, wherein the pre-polymer vapors were guided past the hot filaments which initiated

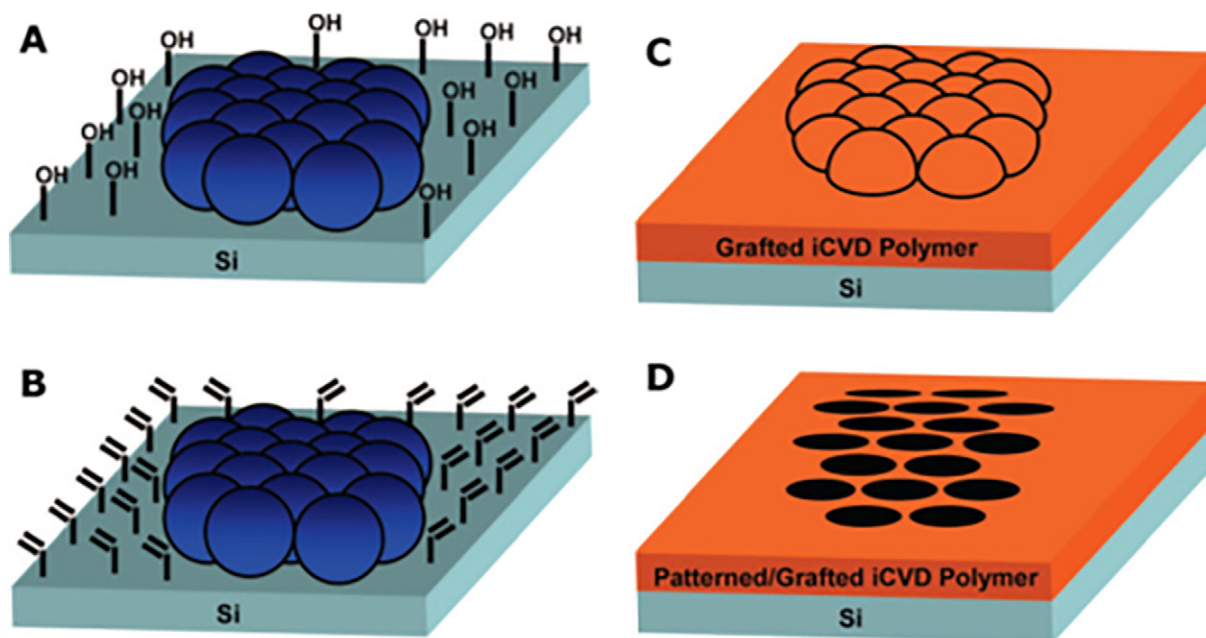


Fig. 9. Colloidal lithography. The four main steps of the method illustrated. (A) Surface after hydroxylation and colloidal mask application, (B) application of vinyl-silane coupling agent, (C) application of polymer film through iCVD method, (D) patterned film after removal of colloidal mask through treatment with Tetrahydrofuran (THF). Adapted with permission from [100]. Copyright 2009 American Chemical Society.

a free radical polymerization process, without the need for a curing agent. As this makes the method non-wetting, it allowed the polymer to infiltrate into the interstices and graft layers starting from the substrate. This resulted in a consistent morphology, as the deposition is not influenced by any capillary effects. Deposition rates between 30 and 200 nm/min could be achieved, depending on polymer being deposited. As polymers are not required to be soluble, and the operating temperature of iCVD is relatively low, certain polymers can be used which are excluded by other CVD techniques. Lastly in the referenced work, the colloidal mask was removed by placing it in a solution of Tetrahydrofuran (THF) and ultra-sonicating it for 10 min. To ensure all colloids were actually removed, the sample was placed in a fresh solution of THF for at least 8 h.

Another example is provided by Kuo and coworkers [102]. They have used gold dots, obtained by double-layer masked CL, as masks for etching silicon wafers by using a reactive ion beam, and fabricated a hexagonal array of silicon nanopillars with diameters as small as 40 nm and aspect ratios as high as seven.

An interesting variation was introduced by Van Duyne and coworkers [103] by depositing materials with a non-zero incident angle. This technique is called angle-resolved colloidal lithography (ARCL) and allows the creation of smaller structures and different geometries.

CL is a new and promising technique for micro- and nanopatterning. Feature sizes can be smaller than 100 nm and the shape can be tuned by changing the crystalline structure of the colloidal crystal mask, the time of anisotropic etching, the incident angle of the vapor beam and the mask registry. This technique, which is a low in cost and high in throughput, can be applied on various material substrates, both planar and curved. However, the polycrystalline nature of the colloidal crystal could be problematic and the presence of defects reduces the patterning precision, especially over large areas. Moreover, producing features below 100 nm dimension is still challenging.

4.2. Mold-replication techniques

Colloidal crystals can be used also as molds for nano imprint lithography, soft lithography and hot or soft embossing. In these cases the colloidal crystal must be anchored to the substrate (for instance by functionalization) and then used directly for the replication into a polymeric material.

Nanoparticle Imprint Lithography (NIL) has been developed by Diao and co-workers [104]. A silicon surface was hydroxylated and 200 μL of a commercially acquired monodisperse colloidal silica suspension was dispersed onto the substrate. A hexagonally close packed monolayer was formed as the substrate engaged with the hydroxyl groups stabilizing the silica particles, resulting in weak hydrogen bonds between the two groups. By sintering, the hydroxyl groups of both substrate and particle were broken, resulting in the silica particles being covalently bonded by an oxygen group to both the substrate and each other. This 'imprint mold' was then used to stamp a pattern into a polymer. To prepare the negative, a glass slide was hydroxylated and treated with a trichlorosilane coupling agent, in order to prevent cracking or peeling of the polymer film. The polymer film consisted out of a prepolymer mixture of polyacrylic acid (monomer), divinylbenzene (crosslinker) and the polymerization initiator IRGACURE 2022. Then the imprint mold was pushed into the prepolymer mixture and cured by subjecting it to ultraviolet light. After lift-off of the mold, spherical pores were found in the polymer film, with diameters from 300 nm down to 15 nm. In a similar fashion, they synthesized iron oxide nanoparticles and used them to make hexagonally shaped pores. The described method and its results are shown in Fig. 10. These pores were then used to study the crystallization of aspirin, which interacted with the polymer film through hydrogen bonding. What they found was that, as long as there were non-curved faces with which the aspirin could align itself, the crystal growth was accelerated, while curved faces impeded the

growth. In fact, the hexagonal pores were the most attractive for the aspirin crystals to grow in.

Choi and co-workers [105] developed an easy method to produce PDMS stamps which could be used with soft lithography techniques to reproduce patterns of colloidal crystals into acrylate films. Self-assembly was performed through a Langmuir-Blodgett method. To prevent cracking, a soluble polymer, polyvinylpyrrolidone (PVP), was added to make the fluid more viscous, reducing the thinning of the depositing meniscus. This also resulted in some of the PVP adhering to the particles, forming small bridges between them which strengthened the physical bonds.

Three variations were presented which allow for the fabrication of a PDMS stamp. A schematic drawing of all three methods and the relations to each other can be seen in Fig. 11. In the first method, the PDMS was deposited on top of the crystal and allowed to infiltrate, after which it was cured for 3 h at 60 °C. After curing the top was peeled off, mechanically separating the polymer matrix in the crystal from that resting on top. Then, a thin layer of acrylate was spin-coated on another glass slide, into which the PDMS stamp was pressed, and cured with UV light. Removal of the stamp revealed the replicated microstructure while the stamp could be reused. In the second method, instead of PDMS the colloidal crystals were infiltrated with a PEDOT:PPS solution. The top layer was etched off with oxygen plasma, leaving behind the pattern which conformed to the bottom of the PS spheres. On top of this a PDMS stamp was developed, producing patterns inverse to the first stamp. The last method involves two steps of self-assembly. On top of the first acrylate pattern a new colloidal self-assembly step was performed, resulting in a spaced monolayer of smaller PS particles. Then, onto this layer a new PDMS stamp is developed.

Another example is provided by Kim and Park [106] who were able to replicate a colloidal crystal into PDMS by means of a soft lithography process. The polymeric substrate was used as a mold to transfer the pattern into polystyrene (PS) thin films by means of hot embossing, the replicated pattern of which shows a hexagonally arrayed structure with few defects.

An additional approach for creating patterns on polymeric substrates is to embed the colloidal crystal into a polymeric matrix and, after dissolving the particles, a pattern of holes can be achieved. Johnson et al [107] applied this technique in order to create an ordered mesoporous polymer by using 35 nm silica spheres. Divinylbenzene (DVB) and ethyleneglycol dimethacrylate (EDMA) were used to fill the pores of the colloidal crystal. After cross-linking the polymers, the particles were dissolved, leaving a polycrystalline network of interconnected pores. This approach is quite reliable and allows for the easy tuning of the dimension of the pores. However, the need to create a colloidal crystal for every single polymeric replica inhibits the process from having a high-throughput and making it unsuitable for industrial applications.

Recently, contact printing has been proposed as a way to transfer a pattern from a colloidal crystal mold to a polymeric substrate. This is not technically considered a mold replication technique since the transferred pattern is created by the colloidal particle themselves. However it is interesting to note that this technique allows well defined structures in the micrometer range to be obtained [108].

5. Conclusion and outlook

This review provides an in-depth look into the large variety of colloidal self-assembly techniques, organized by the type of forces most influencing in the self-assembly process: i) fluidic-based methods, such as Langmuir-Blodgett, dip-coating and droplet evaporation, where the colloidal crystal formation is a result of interaction forces between the particles and their solvent; ii) physical methods, where the self-assembly is governed by shear forces or forces generated by the template, such as spin-coating and confinement methods; iii) the use of external fields, electric or magnetic, used to produce a desired organization of colloidal crystals; and iv) chemical methods, such as template

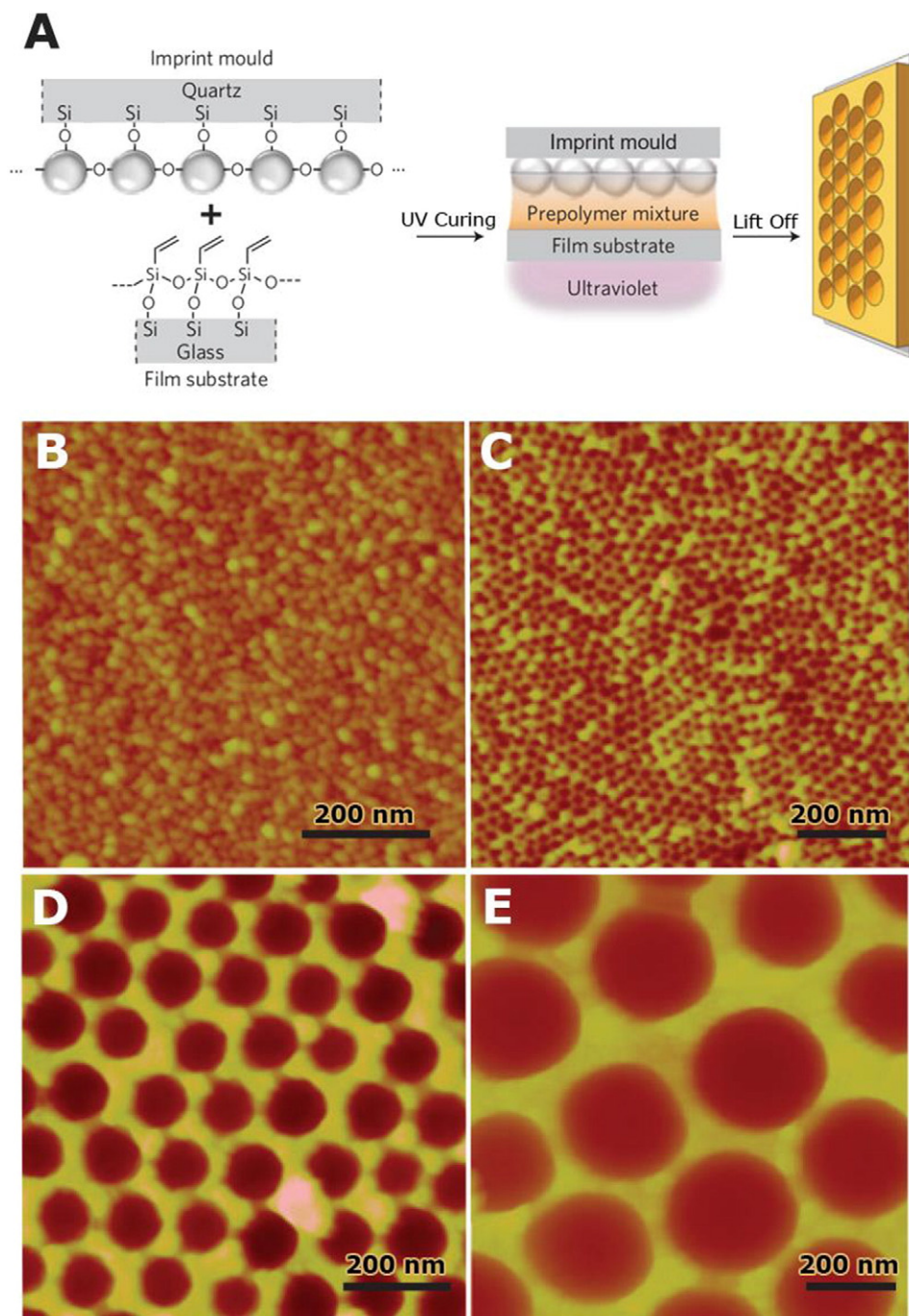


Fig. 10. Nanoparticle imprint lithography. (A) Schematic drawing of production of structured polymer films through a colloidal imprint mold and transparent quartz substrate. AFM images of the pores produced through the imprint method of: (B) 15 nm, (C) 40 nm, (D) 120 nm, (E) 300 nm. Adapted by permission from Macmillan Publishers Ltd.: Nature Materials [104], Copyright 2011.

functionalization or the use of patchy particles, where the self-assembly is controlled by chemical interactions. A last section highlights some examples of how self-assembled colloidal crystals can be used in the patterning of polymeric surfaces by mold-replication methods.

From the comparison of the various approaches for colloidal crystal self-assembly, presented in Table 1, some conclusions can be made as guidelines of which method to pursue depending on the application.

When it comes to the up-scalability of the technique, particularly when thinking of colloidal self-assembly in industrial settings, physical methods are the most promising, as they provide high-throughput and the possibility for large-area structuring. Techniques categorized in this review as physical tend to be well established in current small-

scale manufacturing research and commercial activities, suggesting an ease of implementation of this technology into use.

Using external magnetic or electric fields is favorable when high precision is desired in the final colloidal structures. Mainly due to the accuracy and level of control linked to this self-assembly principle. External fields also provide the means to move away from the surface and extend the concept of colloid crystallinity to the third dimension.

Tuning the chemistry of the colloids' surface offers additional functionalities to these particles, to either control their organization onto a surface or their interaction with each other. For instance, shape-anisotropic particles can provide final structures not possible to achieve

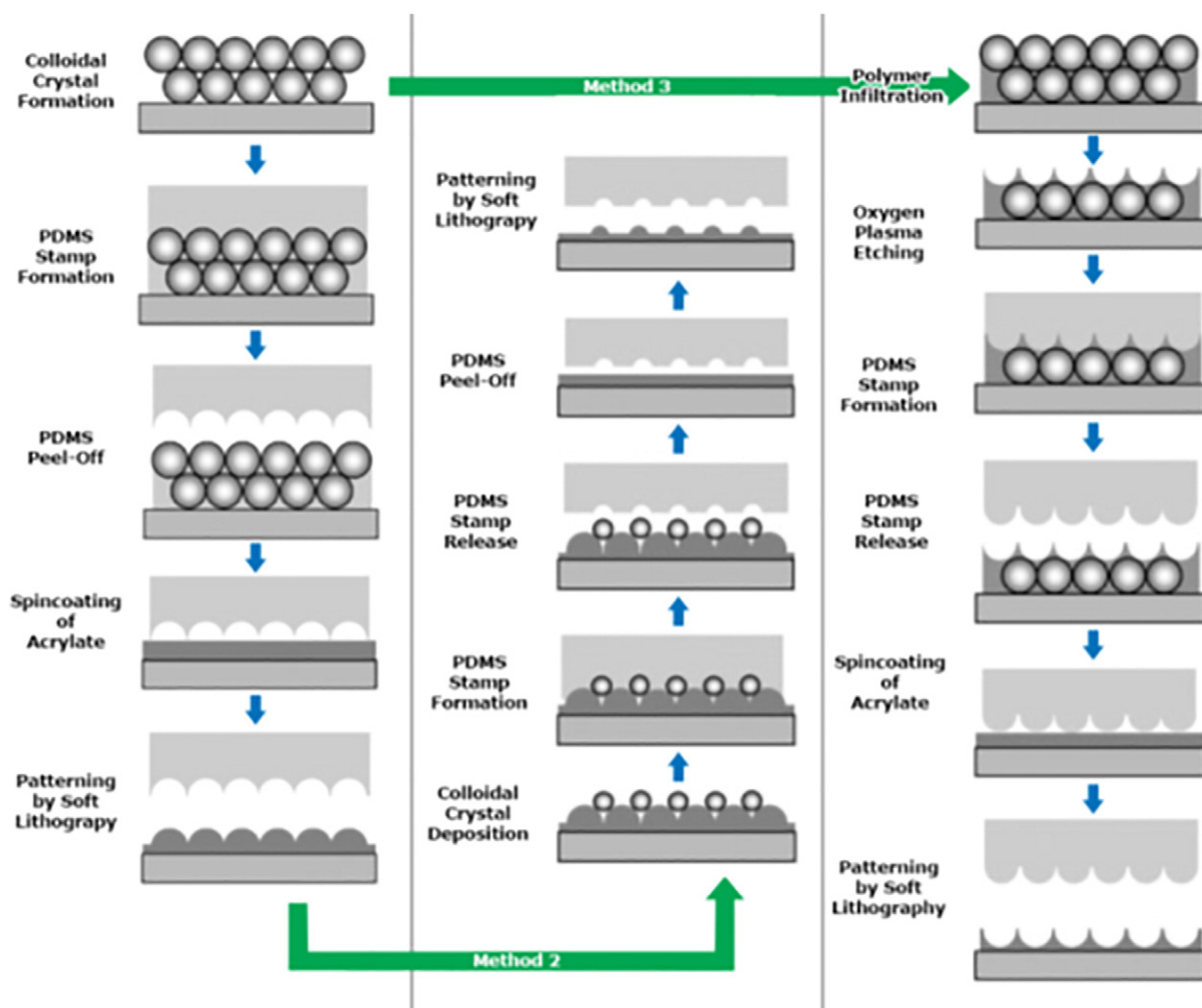


Fig. 11. Soft lithography. Three different methods and their relations to the development of PDMS stamps patterned by colloidal self-assembly. Adapted with permission from [105]. Copyright 2009 WILEY.

with spherical colloids, however they are more difficult to control due to their larger degree of ordering. Although chemical methods offer enormous potential in terms of producing a relatively large influence on colloidal self-assembly via small but effective chemical alterations, these approaches tend to lack when taking into account manufacturing reliability and reproducibility.

Research focused on the realization of colloidal crystals is constantly growing. A particular application is the replication of the colloidal pattern into polymeric substrates. This involves the use of colloidal crystal surfaces as masks (colloidal lithography) or as a mold (for hot embossing, nanoimprint lithography and soft lithography). Therefore, this review set out to provide an overview of recent literature on this topic.

What is important to underline is that, especially for industrial applications, the stability, reproducibility and the total surface area of the pattern are fundamental. For this reason, it is necessary to control the adhesion between the colloidal particles and the substrate. Indeed, immobilization techniques are required to keep the pattern stable by avoiding deformations or even the disruption of the crystal. Several functionalization techniques are already available for the chemical attachment of the particles to the surface (e.g. silanization [109] [110]) or for the embedment of the particles in a polymeric matrix to keep them in place [69].

To make the process scalable and allow for high throughput, another aspect to consider is that the process should be easy and should not

require complex and expensive setups (e.g. controlled magnetic fields). Spin-coating has shown to be a good candidate for obtaining ordered crystals with large monocrystalline domains over large areas.

Regarding the throughput of the replication process, colloidal lithography is not the most suitable technology since it requires the creation of a new colloidal crystal for every substrate. Soft lithography and embossing techniques circumvent this problem. In fact, the colloidal molds could be used several times in order to obtain many polymeric replicas.

The potential for the technologies discussed in this review find relevance in a wide spectrum of application fields, ranging from photonics, catalysis, sensing and control of wetting surface properties [111–115]. The general approach is to exploit the micro- and nano-patterns created via the self-assembly of colloidal crystals to add functionalities deeply linked to the colloidal crystals' topographical properties. Although several options have been discussed in terms of structures and materials made through means of colloidal self-assembly, we believe that this is just the tip of the iceberg, and that future research may reveal new and exciting options to improve previously attained results or introduce novel concepts.

While colloidal crystal self-assembly and its application in micro- and nanopatterning matures into a higher technology readiness level, the growing amount of work dedicated to this topic promises a positive outlook, and the application of these technologies finds space in many fields spanning from photovoltaics to the life sciences.

Table 1
Comparison between self-assembly techniques.

Method			Particle		Self assembly parameters			
Domain	Category	Subcategory	Material	Size [nm]	Solvent(s)	Particle fraction	Time	Temp [°C]
Fluidic	Langmuir-Blodgett	Interface transfer	PS	460–680	DI water / Ethanol	–	–	–
		Draining	PS	200–1000	Water + SDS	10 wt%	–	–
	Dip coating	Meniscus evaporation	PMMA	250–400	DI Water + TEOS	≈0.125 vol%	1–2 [d]	65
		Pipet dispersion	TiO ₂	25	Water + HCl / NaOH	2 vol%	8.1–16 [s]	25.5/10.9
Physical/fluidic	Droplet dispensing	Inkjet nozzle dispersion	SiO ₂	330	Water + DEG + ethylhydroxypropanediol + 2-pyrrolidone	5 wt%	50–2000 [s]	25
Physical	Liquid crystal confinement	Trapping	SiO ₂ /Melamine	3000/3140	5CB	–	–	34.05
		Spincoating	Shear	SiO ₂	100–2000	ETPTA	19.8 vol%	30–960 [s]
		Shear + Humidity adjustment	PS	5000	Water – Ethanol	25/35/45 wt%	<30 [s]	–
			SiO ₂	1500	Ultrapure water	25 wt%	10–30 [s]	–
	Confinement	Surface Patterning	PS	300–800	Water	–	–	55
		Shear and gravity assisted	Doctor blade	SiO ₂	290–560	ETPTA	20–50 wt%	–
Physical/external fields	Field directed spincoating	Shear + AC field	SiO ₂	458	2-Pentanone	20 vol%	–	–
External fields	Alternating electric field	Sheet formation	PS	267	NIPMAm + BIS + SDS + MRB + KPS	1 wt%	103 [s]	20
		Ordering	PS	560–5000	DI water + NaCl	–	<25 [s]	–
Chemical	Static magnetic field	Force balancing	SiO ₂ / Fe ₃ O ₄ – Polymer	1050–5800	Ho(NO ₃) ₃ + DMSO/H ₂ O	–	–	–
		Patchy particles	Kagome lattice	Sulfonated PS	1000	DI Water + NaCl	–	≈ 15 [h]
	Template functionalization	Selective functionalization	SiO ₂	2000	Water	–	–	–
		Surface treatment	SiO ₂	67	Ethanol / Water	2.04 wt%	1.5 [h]	–
	DNA functionalization	Crystallization	PS/PMMA/Silica/TPM	540/1000/1500	PBS	1 wt%	45 [h]	27–28.3

^a Stb, Unst and Cond are abbreviations for Stable, Unstable and Conditionally stable, respectively.

Table 1 (continued)

Method	Self assembly parameters		Functionalization		Crystalline properties			
	Stability ^a	Substrate	Substrate	Particle	Structure	Ordering	Crystallinity	Ref
Fluidic	Stb	Glass	Allyltrimethoxysilane (HL)	None	Mono/multi	CP/HCP	Poly	[61]
	Stb	Si / Glass	None	None	Mono/binary	CP	Mono	[62]
	Stb	Si / Glass	None	None	Multi	HCP	Mono	[63]
	Stb	Glass	None	None	Ringlike	–	–	[66]
	Stb	Si / Cu / PDMS	Si: OTS (HH)	None	Multi	HCP	Poly	[67]
Physical/fluidic	Stb	Glass	None	DMOAP	Single	–	–	[79]
	Stb	Si	APTCS	None	Mono/multi	CP/HCP	Poly	[70,71]
	Stb	Glass	None	None	Mono	CP	Incomplete	[72]
	Stb	Glass	None	None	Mono	CP	Poly	[73]
	Stb	Glass + Azoaromatic Polymer	None	None	Mono	Stripes/CR/CP	Poly	[74]
Physical/external fields	Stb	Glass	None	None	Multi	CP	Poly	[82]
	Stb	Glass	None	None	Mono	CP	Poly	[85]
	Unst	Glass / ITO	None	None	Mono	Tubular/Sheet	–	[83]
	Unst	Glass / ITO	None	None	Mono	Oligomer	–	[84]
	Cond	PDMS / Ni	TPI	SiO ₂ ; NH ₂ / Fe ₃ O ₄ – Polymer: COOH / RITC	Mono 3D	Structured	–	[86]
Chemical	Unst	SiO ₂	–	Ti + Au	Mono	Kagome	–	[91]
	Unst	Glass	None	Ti + Au	Mono	“K”/“Y”/“X”	–	[92]
	Stb	Si	APTCS	None	Mono	Aggregate	–	[58]
	Cond	Glass	HMDS (HH)	Azide + DNA	3D/Bbinary	FCC/CsCl/AlB ₂ /Cs ₆ C ₆₀	Poly	[96]

Acknowledgments

This research received no specific grant from any funding agency in the public, commercial, or not-for-profit sectors.

References

- Xia Y, Whitesides GM. Soft lithography. *Annu Rev Mater Sci* 1998;28:153–84. <https://doi.org/10.1146/annurev.matsci.28.1.153>.
- Fanzio P, Mussi V, Manneschi C, Angeli E, Firpo G, Repetto L, et al. DNA detection with a polymeric nanochannel device. *Lab Chip* 2011;11:2961. <https://doi.org/10.1039/c1lc20243j>.
- Becker H, Heim U. Hot embossing as a method for the fabrication of polymer high aspect ratio structures. *Sensors Actuators A Phys* 2000;83:130–5. [https://doi.org/10.1016/S0924-4247\(00\)00296-X](https://doi.org/10.1016/S0924-4247(00)00296-X).
- Peng L, Deng Y, Yi P, Lai X. Micro hot embossing of thermoplastic polymers: a review. *J Micromech Microeng* 2014;24:13001. <https://doi.org/10.1088/0960-1317/24/1/013001>.
- Fanzio P, Cagliani A, Peterffy KG, Sasso L. High throughput soft embossing process for micro-patterning of PEDOT thin films. *Microelectron Eng* 2017;176:15–21. <https://doi.org/10.1016/j.mee.2017.01.011>.
- Guo LJ. Nanoimprint lithography: methods and material requirements. *Adv Mater* 2007;19:495–513. <https://doi.org/10.1002/adma.200600882>.
- Schift H. Nanoimprint lithography: an old story in modern times? A review. *J Vac Sci Technol B: Microelectron Nanometer Struct* 2008;26:458. <https://doi.org/10.1116/1.2890972>.
- Gates Byron D, Xu Qiaobing, Stewart Michael, Ryan Declan, Grant Willson C, Whitesides George M. New approaches to nanofabrication: molding, printing, and other techniques; 2005. <https://doi.org/10.1021/CR0300760>.
- Park W, Rhie J, Kim NY, Hong S, Kim D-S. Sub-10 nm feature chromium photo-masks for contact lithography patterning of square metal ring arrays. *Sci Rep* 2016;6:23823. <https://doi.org/10.1038/srep23823>.
- Reyntjens S, Puers R. A review of focused ion beam applications in microsystem technology. *J Micromech Microeng* 2001;11:287–300. <https://doi.org/10.1088/0960-1317/11/4/301>.
- Mussi V, Fanzio P, Repetto L, Firpo G, Valbusa U, Scaruffi P, et al. Solid state nanopores for gene expression profiling. *Superlattice Microsc* 2009;46:59–63. <https://doi.org/10.1016/j.spmi.2008.09.003>.
- Deubel M, von Freymann G, Wegener M, Pereira S, Busch K, Soukoulis CM. Direct laser writing of three-dimensional photonic-crystal templates for telecommunications. *Nat Mater* 2004;3(7):444. <https://doi.org/10.1038/nmat1155>.
- LaFratta C, Baldacchini T. Two-photon polymerization metrology: characterization methods of mechanisms and microstructures. *Micromachines* 2017;8:101. <https://doi.org/10.3390/mi8040101>.
- Whitesides GM, Grzybowski B. Self-assembly at all scales. *Science* 2002;295:2418–21. <https://doi.org/10.1126/science.1070821>.
- Vogel N, Retsch M, Fustin CA, Del Campo A, Jonas U. Advances in colloidal assembly: the design of structure and hierarchy in two and three dimensions. *Chem Rev* 2015;115:6265–311. <https://doi.org/10.1021/cr400081d>.
- Zhang J, Yang B. Patterning colloidal crystals and nanostructure arrays by soft lithography. *Adv Funct Mater* 2010;20:3411–24. <https://doi.org/10.1002/adfm.201000795>.
- Matijevic E. Uniform inorganic colloid dispersions. Achievements and challenges. *Langmuir* 1994;10:8–16. <https://doi.org/10.1021/la00013a003>.
- Matijevic E. Preparation and properties of uniform size colloids. *Chem Mater* 1993;5:412–26. <https://doi.org/10.1021/cm00028a004>.
- Matijevic E. Monodispersed metal (hydrous) oxides - a fascinating field of colloid science. *Acc Chem Res* 1981;14:22–9. <https://doi.org/10.1021/ar00061a004>.
- Grzelczak M, Vermant J, Furst EM, Liz-Marzán LM. Directed self-assembly of nanoparticles. *ACS Nano* 2010;4:3591–605. <https://doi.org/10.1021/nn100869j>.
- Guerrero-Martínez A, Pérez-Juste J, Liz-Marzán LM. Recent progress on silica coating of nanoparticles and related nanomaterials. *Adv Mater* 2010;22:1182–95. <https://doi.org/10.1002/adma.200901263>.
- Wang J, Shah ZH, Zhang S, Lu R, J-G Xu, Wang X-R, et al. Silica-based nanocomposites via reverse microemulsions: classifications, preparations, and applications. *Nanoscale* 2014;6:4418. <https://doi.org/10.1039/c3nr06025j>.
- Liberman A, Mendez N, Trogler WC, Kummel AC. Synthesis and surface functionalization of silica nanoparticles for nanomedicine. *Surf Sci Rep* 2014;69:132–58. <https://doi.org/10.1016/j.surfrep.2014.07.001>.
- Hyde EDER, Seyfaee A, Neville F, Moreno-Atanasio R. Colloidal silica particle synthesis and future industrial manufacturing pathways: a review. *Ind Eng Chem Res* 2016;55:8891–913. <https://doi.org/10.1021/acs.iecr.6b01839>.
- R a Sperling, Parak WJ. Surface modification, functionalization and bioconjugation of colloidal inorganic nanoparticles. *Philos Transact A Math Phys Eng Sci* 2010;368:1333–83. <https://doi.org/10.1098/rsta.2009.0273>.
- Birdi KS. *Handbook of surface and colloid chemistry*. Third. CRC Press; 2009.
- Walther A, Müller AHE. Janus particles: synthesis, self-assembly, physical properties, and applications. *Chem Rev* 2013;113:5194–261. <https://doi.org/10.1021/cr300089t>.
- Kaewsanaha C, Tangboriboonrat P, Polpanich D, Eissa M, Elaissari A. Janus colloidal particles: preparation, properties, and biomedical applications. *ACS Appl Mater Interfaces* 2013;5:1857–69.
- Pawar AB, Kretzschmar I. Patchy particles by glancing angle deposition. *Langmuir* 2008;24:355–8. <https://doi.org/10.1021/la703005z>.
- Pawar AB, Kretzschmar I. Multifunctional patchy particles by glancing angle deposition. *Langmuir* 2009;25:9057–63. <https://doi.org/10.1021/la900809b>.
- Lotito V, Zambelli T. Approaches to self-assembly of colloidal monolayers: a guide for nanotechnologists. *Adv Colloid Interf Sci* 2017;246:217–74. <https://doi.org/10.1016/j.cis.2017.04.003>.
- Li Q, Jonas U, Zhao XS, Kappl M. The forces at work in colloidal self-assembly: a review on fundamental interactions between colloidal particles. *Asia Pac J Chem Eng* 2008;3:255–68. <https://doi.org/10.1002/apj.144>.
- Bishop KJM, Wilmer CE, Soh S, Grzybowski BA. Nanoscale forces and their uses in self-assembly. *Small* 2009;5:1600–30. <https://doi.org/10.1002/smll.200900358>.
- Ninham BW, Lo Nostro P. *Molecular forces and self assembly*. Colloid, nano sciences and biology. Cambridge University Press; 2010.
- Hwang RQ, Pohl K, Bartelt MC, de la Figuera J, Bartelt NC, Hrbek J. Identifying the forces responsible for self-organization of nanostructures at crystal surfaces. *Nature* 1999;397:238–41. <https://doi.org/10.1038/16667>.
- Vold MJ. The effect of adsorption on the van der waals interaction of spherical colloidal particles. *J Colloid Sci* 1961;16:1–12. [https://doi.org/10.1016/0095-8522\(61\)90057-5](https://doi.org/10.1016/0095-8522(61)90057-5).
- Kim HY, Sofo JO, Velegol D, Cole MW, Lucas AA. Van der waals dispersion forces between dielectric nanoclusters. *Langmuir* 2007;23:1735–40. <https://doi.org/10.1021/la061802w>.
- Moncho-Jordá A, Martínez-López F, González AE, Hidalgo-Álvarez R. Role of long-range repulsive interactions in two-dimensional colloidal aggregation: experiments and simulations; 2002. <https://doi.org/10.1021/LA0258805>.
- Stamou, Duschl, Johannsmann. Long-range attraction between colloidal spheres at the air-water interface: the consequence of an irregular meniscus. *Phys Rev E Stat Phys Plasmas Fluids Relat Interdiscip Topics* 2000;62:5263–72.
- Min Y, Akbulut M, Kristiansen K, Golan Y, I J. The role of Interparticle and external forces in nanoparticle assembly. *Nat Mater* 2008;7:527–38. <https://doi.org/10.1038/nmat2206>.
- McCorty R, Fung J, Kaz D, Manoharan VN. Colloidal self-assembly at an interface. *Mater Today* 2010;13:34–42. [https://doi.org/10.1016/S1369-7021\(10\)70107-3](https://doi.org/10.1016/S1369-7021(10)70107-3).
- Bendersky M, Davis JM. DLVO interaction of colloidal particles with topographically and chemically heterogeneous surfaces. *J Colloid Interface Sci* 2011;353:87–97. <https://doi.org/10.1016/j.jcis.2010.09.058>.
- Ohshima H. *Electrical phenomena at interfaces and biointerfaces: fundamentals and applications in nano-, bio-, and environmental sciences*. Wiley; 2012.
- Hoek EMV, Agarwal GK. Extended DLVO interactions between spherical particles and rough surfaces. *J Colloid Interface Sci* 2006;298:50–8. <https://doi.org/10.1016/j.jcis.2005.12.031>.
- Sacanna S, Pine DJ, Yi G-R. Engineering shape: the novel geometries of colloidal self-assembly. *Soft Matter* 2013;9:8096–106. <https://doi.org/10.1039/c3sm55000f>.
- Schwartz MM. *New materials, processes, and methods technology*. Taylor & Francis; 2006.
- Timp GL. *Nanotechnology*. AIP Press; 1999.
- Brinker JC, Lu Y, Sellinger A, Fan H. Evaporation-induced self-assembly: nanostructures made easy. *Adv Mater* 1999;11:579–85. [https://doi.org/10.1002/\(SICI\)1521-4095\(199905\)11](https://doi.org/10.1002/(SICI)1521-4095(199905)11).
- Syms RRA, Yeatman EM, Bright VM, Whitesides GM. Surface tension-powered self-assembly of microstructures - the state-of-the-art. *J Microelectromech Syst* 2003;12:387–417. <https://doi.org/10.1109/JMEMS.2003.811724>.
- Hu L, Chen M, Fang X, Wu L. Oil-water interfacial self-assembly: a novel strategy for nanofilm and nanodevice fabrication. *Chem Soc Rev* 2012;41:1350. <https://doi.org/10.1039/c1cs15189d>.
- Vogel N, Weiss CK, Landfester K, Kessler H, Schwarz US, Spatz JP, et al. From soft to hard: the generation of functional and complex colloidal monolayers for nanolithography. *Soft Matter* 2012;8:4044–61. <https://doi.org/10.1039/C1SM06650A>.
- Dugyala VR, Daware SV, Basavaraj MG. Shape anisotropic colloids: synthesis, packing behavior, evaporation driven assembly, and their application in emulsion stabilization. *Soft Matter* 2013;9:6711–25. <https://doi.org/10.1039/c3sm550404b>.
- Castillo-León J, Sasso L, Svendsen WE. Self-assembled peptide nanostructures: advances and applications in nanobiotechnology. *ACS Nano* 2013;7:1030–1039. <https://doi.org/10.1021/nl300110a004>.
- Wang PY, Shields CW, Zhao T, Jami H, López GP, Kingshott P. Rapid self-assembly of shaped microtubes into large, close-packed crystalline monolayers on solid surfaces. *Small* 2016;12:1309–14. <https://doi.org/10.1002/smll.201503130>.
- Zhang S-Y, Regulacio MD, Han M-Y. Self-assembly of colloidal one-dimensional nanocrystals. *Chem Soc Rev* 2014;43:2301. <https://doi.org/10.1039/c3cs60397k>.
- Woodcock LV. Entropy difference between the face-centred cubic and hexagonal close-packed crystal structures. *Nature* 1997;385:141–3. <https://doi.org/10.1038/385141a0>.
- Li X, Niitsoo O, Couzis A. Electrostatically driven adsorption of silica nanoparticles on functionalized surfaces. *J Colloid Interface Sci* 2013;394:26–35. <https://doi.org/10.1016/j.jcis.2012.11.042>.
- Zhang J, Sun Z, Yang B. Self-assembly of photonic crystals from polymer colloids. *Curr Opin Colloid Interface Sci* 2009;14:103–14. <https://doi.org/10.1016/j.cocis.2008.09.001>.
- Petty MC. *Langmuir-Blodgett films: an introduction*. Cambridge University Press; 1996.
- Reculosa S, Ravaine S. Synthesis of colloidal crystals of controllable thickness through the Langmuir-Blodgett technique. *Chem Mater* 2003;15:598–605. <https://doi.org/10.1021/cm021242w>.
- Lotito V, Zambelli T. Self-assembly of single sized and binary colloidal particles at air/water interface by surface confinement and water discharge. *Langmuir* 2016. <https://doi.org/10.1021/acs.langmuir.6b02157>.
- Hatton B, Mishchenko L, Davis S, Sandhage KH, Aizenberg J. Assembly of large-area, highly ordered, crack-free inverse opal films. *Proc Natl Acad Sci U S A* 2010;107:10354–9. <https://doi.org/10.1073/pnas.1000954107>.

- [63] Maki KL, Kumar S. Fast evaporation of spreading droplets of colloidal suspensions. *Langmuir* 2011;27:11347–63. <https://doi.org/10.1021/la202088s>.
- [64] Deegan RD, Bakajin O, Dupont TF, Huber G, Nagel SR, Witten TA. Capillary flow as the cause of ring stains from dried liquid drops. *Nature* 1997;389:827–9. <https://doi.org/10.1038/39827>.
- [65] Bhardwaj R, Fang X, Somasundaran P, Attinger D. Self-assembly of colloidal particles from evaporating droplets: role of DLVO interactions and proposition of a phase diagram. *Langmuir* 2010;26:7833–42. <https://doi.org/10.1021/la9047227>.
- [66] Ko H, Park J, Shin H, Moon J. Rapid self-assembly of monodisperse colloidal spheres in an ink-jet printed droplet. The ability of monodisperse colloidal spheres to self-assemble into crystalline arrays makes them interesting and versatile building blocks for advanced materials. *High Chem Mater* 2004;189:4212–5. <https://doi.org/10.1021/cm035256t>.
- [67] Majumder M, Rendall CS, Eukel JA, Wang JYL, Behabtu N, Pint CL, et al. Overcoming the “coffee-stain” effect by compositional marangoni-flow-assisted drop-drying. *J Phys Chem B* 2012;116:6536–42. <https://doi.org/10.1021/jp3009628>.
- [68] Hall DB, Underhill P, Torkelson JM. Spin coating of thin and ultrathin polymer films. *Polym Eng Sci* 1998;38:2039–45. <https://doi.org/10.1002/pen.10373>.
- [69] Jiang P, McFarland MJ. Large-scale fabrication of wafer-size colloidal crystals, macroporous polymers and nanocomposites by spin-coating. *J Am Chem Soc* 2004;126:13778–86. <https://doi.org/10.1021/ja0470923>.
- [70] Jiang P, Prasad T, McFarland MJ, Colvin VL. Two-dimensional nonclose-packed colloidal crystals formed by spincoating. *Appl Phys Lett* 2006;89:2004–7. <https://doi.org/10.1063/1.2218832>.
- [71] Toolan DTW, Fujii S, Ebbens SJ, Nakamura Y, Howse JR. On the mechanisms of colloidal self-assembly during spin-coating. *Soft Matter* 2014;10:8804–12. <https://doi.org/10.1039/C4SM01711K>.
- [72] Cheng Y, Jönsson PG, Zhao Z. Controllable fabrication of large-area 2D colloidal crystal masks with large size defect-free domains based on statistical experimental design. *Appl Surf Sci* 2014;313:144–51. <https://doi.org/10.1016/j.apsusc.2014.05.167>.
- [73] Ye YH, Badilescu S, Van Truong V, Rochon P, Natansohn A. Self-assembly of colloidal spheres on patterned substrates. *Appl Phys Lett* 2001;79:872–4. <https://doi.org/10.1063/1.1391234>.
- [74] Xia D, Biswas A, Li D, Brueck SRJ. Directed self-assembly of silica nanoparticles into nanometer-scale patterned surfaces using spin-coating. *Adv Mater* 2004;16:1427–32. <https://doi.org/10.1002/adma.200400095>.
- [75] Asbahi M, Wang F, Dong Z, Yang JKW, Chong KSL. Directed self-assembly of sub-10 nm particle clusters using topographical templates. *Nanotechnology* 2016;27:424001. <https://doi.org/10.1088/0957-4484/27/42/424001>.
- [76] Asbahi M, Wang F, Dong Z, Yang JKW, Chong KSL. Directed self-assembly of sub-10 nm particle clusters using topographical templates. *Nanotechnology* 2016;27:424001. <https://doi.org/10.1088/0957-4484/27/42/424001>.
- [77] Zhao JJ, Duan YY, Wang XD, Wang BX. Effect of nanofluids on thin film evaporation in microchannels. *J Nanopart Res* 2011;13:5033–47. <https://doi.org/10.1007/s11051-011-0484-y>.
- [78] Silvestre NM, Liu Q, Senyuk B, Smalyukh II, Tasinkevych M. Towards template-assisted assembly of nematic colloids. *Phys Rev Lett* 2014;112:1–5. <https://doi.org/10.1103/PhysRevLett.112.225501>.
- [79] Tasinkevych M, Silvestre NM, Telo Da Gama MM. Liquid crystal boojum-colloids. *New J Phys* 2012;14. <https://doi.org/10.1088/1367-2630/14/7/073030>.
- [80] Lubensky TC, Petey D, Currier N, Stark H. Topological defects and interactions in nematic emulsions. *Phys Rev E* 1997;57:610–25. <https://doi.org/10.1103/PhysRevE.57.610>.
- [81] Yang H, Jiang P. Large-scale colloidal self-assembly by doctor blade coating. *Langmuir* 2010;26:13173–82. <https://doi.org/10.1021/la101721v>.
- [82] Crassous JJ, Mihut AM, Wernersson E, Pfeleiderer P, Vermant J, Linse P, et al. Field-induced assembly of colloidal ellipsoids into well-defined microtubules. *Nat Commun* 2014;5:5516. <https://doi.org/10.1038/ncomms6516>.
- [83] Ma F, DT Wu, Wu N. Formation of colloidal molecules induced by alternating-current electric fields. *J Am Chem Soc* 2013;135:6–9.
- [84] Bartlett AP, Pichumani M, Giuliani M, González-Viñas W, Yethiraj A. Modified spin-coating technique to achieve directional colloidal crystallization. *Langmuir* 2012;28:3067–70. <https://doi.org/10.1021/la204123s>.
- [85] Demirörs AF, Pillai PP, Kowalczyk B, B a Grzybowski. Colloidal assembly directed by virtual magnetic moulds. *Nature* 2013;2:3–7. <https://doi.org/10.1038/nature12591>.
- [86] Tipler PA, Mosca G. Physics for scientists and engineers. W.H. Freeman; 2008.
- [87] Zhang Glotzer SC. Self-assembly of patchy particles. *Nano Lett* 2004;4:1407–13. <https://doi.org/10.1021/nl0493500>.
- [88] Romano F, Sciortino F. Colloidal self-assembly: patchy from the bottom up. *Nat Mater* 2011;10(3):171. <https://doi.org/10.1038/nmat2975>.
- [89] Romano F, Sciortino F, Pastore G, Noya EG, Stradner A, Schurtenberger P, et al. Two dimensional assembly of triblock Janus particles into crystal phases in the two bond per patch limit. *Soft Matter* 2011;7:5799. <https://doi.org/10.1039/c0sm01494j>.
- [90] Chen Q, Bae SC, Granick S. Directed self-assembly of a colloidal kagome lattice. *Nature* 2011;469:381–4. <https://doi.org/10.1038/nature09713>.
- [91] Chen Q, Diesel E, Whitmer JK, Bae SC, Luijten E, Granick S. Triblock colloids for directed self-assembly. *J Am Chem Soc* 2011;133:7725–7. <https://doi.org/10.1021/ja202360g>.
- [92] Li H, Carter JD, LaBeau TH. Nanofabrication by DNA self-assembly. *Mater Today* 2009;12:24–32. [https://doi.org/10.1016/S1369-7021\(09\)70157-9](https://doi.org/10.1016/S1369-7021(09)70157-9).
- [93] Le John D, Pinto Yariv, Seeman Nadrian C, Musier-Forsyth Karin, Andrew Taton T, Kiehl Richard A. DNA-Templated self-assembly of metallic nanocomponent arrays on a surface; 2004. <https://doi.org/10.1021/NL048635+>.
- [94] Zheng J, Constantinou PE, Micheel C, Alivisatos AP, Kiehl RA, Seeman NC. Two-dimensional nanoparticle arrays show the organizational power of robust DNA motifs. *Nano Lett* 2006;6:1502–4. <https://doi.org/10.1021/nl060994c>.
- [95] Wang Y, Wang Y, Zheng X, Ducrot É, Yodh JS, Weck M, et al. Crystallization of DNA-coated colloids. *Nat Commun* 2015;6:7253. <https://doi.org/10.1038/ncomms8253>.
- [96] Park M, Chaikin PM, Register RA, Adamson DH. Large area dense nanoscale patterning of arbitrary surfaces. *Appl Phys Lett* 2001;79:257–9. <https://doi.org/10.1063/1.1378046>.
- [97] Zhang G, Wang D. Colloidal lithography - the art of nanochemical patterning. *Chem Asian J* 2009;4:236–45. <https://doi.org/10.1002/asia.200800298>.
- [98] Wood MA. Colloidal lithography and current fabrication techniques producing in-plane nanotopography for biological applications. *J R Soc Interface* 2007;4:1–17. <https://doi.org/10.1098/rsif.2006.0149>.
- [99] Choi Dae-Geun, Yu Hyung Kyun, Jang Se Gyu, Yang S-M. Colloidal lithographic nanopatterning via reactive ion etching; 2004. <https://doi.org/10.1021/JA0319083>.
- [100] Trujillo NJ, Baxamusa SH, Gleason KK. Grafted functional polymer nanostructures patterned bottom-up by colloidal lithography and initiated chemical vapor deposition (iCVD). *Chem Mater* 2009;21:742–50. <https://doi.org/10.1021/cm803008r>.
- [101] Tenhaeff WE, Gleason KK. Initiated and oxidative chemical vapor deposition of polymeric thin films: ICVD and oCVD. *Adv Funct Mater* 2008;18:979–92. <https://doi.org/10.1002/adfm.200701479>.
- [102] Kuo Chun-Wen, Shiu Jau-Ye, Chen Peilin, Somorjai Gabor A. Fabrication of size-tunable large-area periodic silicon nanopillar arrays with Sub-10-nm resolution; 2003. <https://doi.org/10.1021/JP035468D>.
- [103] Haynes Christy L, McFarland Adam D, Smith Matthew T, Hulteen John C, Van Duyne RP. Angle-resolved nanosphere lithography: manipulation of nanoparticle size, shape, and interparticle spacing; 2002. <https://doi.org/10.1021/JP013570+>.
- [104] Diao Y, Harada T, Myerson AS, Hatton TA, Trout BL. The role of nanopore shape in surface-induced crystallization. *Nat Mater* 2011;10:867–71. <https://doi.org/10.1038/nmat3117>.
- [105] Choi HK, Kim MH, Im SH, Park OO. Fabrication of ordered nanostructured arrays using poly(dimethylsiloxane) replica molds based on three-dimensional colloidal crystals. *Adv Funct Mater* 2009;19:1594–600. <https://doi.org/10.1002/adfm.200801096>.
- [106] Kim MH, Park OO. Hot embossing of polymeric nanostructures using poly(dimethylsiloxane) replica molds based on three-dimensional colloidal crystals. *Microelectron Eng* 2012;91:121–6. <https://doi.org/10.1016/j.mee.2011.11.007>.
- [107] Johnson SA, Olivier PJ, Mallouk TE. Ordered mesoporous polymers of tunable pore size from colloidal silica templates. *Science* 1999;283:963–5. <https://doi.org/10.1126/science.283.5404.963>.
- [108] Yan Xin, Yao Jimin, Lu Guang, Chen Xin, Zhang Kai, Yang Bai. Microcontact printing of colloidal crystals; 2004. <https://doi.org/10.1021/JA0479078>.
- [109] Wood MA, Meredith DO, Owen GR. Steps toward a model nanotopography. *IEEE Trans Nanobioscience* 2002;1:133–40.
- [110] Sato T. Nanoscale colloidal particles: monolayer organization and patterning. *J Vac Sci Technol B: Microelectron Nanometer Struct* 1997;15:45. <https://doi.org/10.1116/1.589253>.
- [111] Marlow F, Muldarisnur Sharifi P, Brinkmann R, Mendive C. Opals: status and prospects. *Angew Chem Int Ed* 2009;48:6212–33. <https://doi.org/10.1002/anie.200900210>.
- [112] Moon JH, Yang S. Chemical aspects of three-dimensional photonic crystals. *Chem Rev* 2010;110:547–74. <https://doi.org/10.1021/cr900080v>.
- [113] Aguirre CI, Reguera E, Stein A. Tunable colors in opals and inverse opal photonic crystals. *Adv Funct Mater* 2010;20:2565–78. <https://doi.org/10.1002/adfm.201000143>.
- [114] Ge J, Yin Y. Responsive photonic crystals. *Angew Chem Int Ed* 2011;50:1492–522. <https://doi.org/10.1002/anie.200907091>.
- [115] Wang J, Zhang Y, Wang S, Song Y, Jiang L. Bioinspired colloidal photonic crystals with controllable wettability. *Acc Chem Res* 2011;44:405–15. <https://doi.org/10.1021/ar1001236>.